Molecular Therapy
Original Article

PDE10A Inhibition Reduces the Manifestation of Pathology in DMD Zebrafish and Represses the Genetic Modifier PITPNA

Matthias R. Lambert,[1,2] Janelle M. Spinazzola,[1,2] Jeffrey J. Widrick,[1,2] Anna Pakula,[1,2] James R. Conner,[1,2] Janice E. Chin,[6] Jane M. Owens,[6] and Louis M. Kunkel[1,2,3,4,5]

[1]Division of Genetics and Genomics, Boston Children's Hospital, Boston, MA 02115, USA; [2]Department of Pediatrics, Harvard Medical School, Boston, MA 02115, USA; [3]The Stem Cell Program, Boston Children's Hospital, Boston, MA 02115, USA; [4]Harvard Stem Cell Institute, Cambridge, MA 02138, USA; [5]The Manton Center for Orphan Disease Research at Boston Children's Hospital, Boston, MA 02115, USA; [6]Rare Disease Research Unit, Pfizer, Cambridge, MA 02139, USA

Duchenne muscular dystrophy (DMD) is a severe genetic disorder caused by mutations in the *DMD* gene. Absence of dystrophin protein leads to progressive degradation of skeletal and cardiac function and leads to premature death. Over the years, zebrafish have been increasingly used for studying DMD and are a powerful tool for drug discovery and therapeutic development.

In our study, a birefringence screening assay led to identification of phosphodiesterase 10A (PDE10A) inhibitors that reduced the manifestation of dystrophic muscle phenotype in dystrophin-deficient *sapje-like* zebrafish larvae. PDE10A has been validated as a therapeutic target by *pde10a* morpholino-mediated reduction in muscle pathology and improvement in locomotion, muscle, and vascular function as well as long-term survival in *sapje-like* larvae. PDE10A inhibition in zebrafish and DMD patient-derived myoblasts were also associated with reduction of *PITPNA* expression that has been previously identified as a protective genetic modifier in two exceptional dystrophin-deficient golden retriever muscular dystrophy (GRMD) dogs that escaped the dystrophic phenotype. The combination of a phenotypic assay and relevant functional assessments in the *sapje-like* zebrafish enhances the potential for the prospective discovery of DMD therapeutics. Indeed, our results suggest a new application for a PDE10A inhibitor as a potential DMD therapeutic to be investigated in a mouse model of DMD.

INTRODUCTION

Duchenne muscular dystrophy (DMD) is a progressive and severe recessive genetic disorder caused by mutations in the *DMD* gene[1,2] that lead to the absence of functional dystrophin protein.[3] Dystrophin is an integral part of the dystrophin-associated glycoprotein complex (DAPC) at the sarcolemma[4,5] that provides structural stability and a signaling anchor to the muscle fibers.[6,7] In the context of dystrophin loss, muscle fibers become more susceptible to contraction-induced injuries,[8] which exacerbate sarcolemma permeability and give rise to a cascade of inflammatory and impaired regenerative capacity events, causing progressive necrosis of the fibers and their replacement by connective tissue and fat (for reviews, see Guiraud et al.[6] and Allen et al.[7]).

Approximately 1 in 5,000 newborn boys is affected by DMD.[9,10] Patients living with DMD start to typically show a gradual decline of muscle function in the first decade of age,[11,12] and most develop cardiovascular complications in the second decade, which is one of the main causes of premature death besides respiratory failure.[7,13] The recent advances in whole-genome/exome sequencing and the use of large-scale databases have enabled the identification of several genetic modifiers that influence clinical presentation of the disease (for review, see Hightower and Alexander[14]). Variants in the *SPP1*,[15] *LTBP4*,[16,17] *CD40*,[18] *ACTN3*,[19] and *TCTEX1D1* genes[20] were associated with age of ambulation loss and muscle function in patients with DMD. Moreover, the use of animal models including dystrophin-deficient mice led to additional identification of genetic modifiers and respective mechanisms of action that impact secondary pathways of the disease.[21–27] In our laboratory, *Jagged1* and *Pitpna* were revealed from the study of two exceptional *escaper* golden retriever muscular dystrophy (GRMD) dogs that exhibited a very mild phenotype.[28,29] Ringo and his descendant Suflair displayed histological features of the dystrophic process, but they remained fully ambulatory with a normal lifespan and they were able to breed naturally without compensatory upregulation of the structurally similar protein utrophin.[30,31] This striking story raised the paradigm shift that large muscles can be partially functional despite the absence of muscle dystrophin.[32] Both *escaper* dogs showed an overexpression of *Jagged1* due to a naturally occurring variant in its promoter, and an improvement of *in vitro* myogenic regenerative capacities.[28] Further microarray analysis of muscle also revealed *Pitpna* as the only exclusive gene differentially expressed between *escaper* and

Received 3 August 2020; accepted 15 November 2020;
https://doi.org/10.1016/j.ymthe.2020.11.021.

Correspondence: Louis M. Kunkel, Division of Genetics and Genomics, Boston Children's Hospital, 3 Blackfan Circle, Boston, MA 02115, USA.
E-mail: kunkel@enders.tch.harvard.edu

severely affected dogs.[29] *PITPNA* downregulation enhanced the formation of mature myotubes in DMD patient-derived muscle cells, while it restored muscle phenotype and prolonged the survival of dystrophin-deficient zebrafish (*Danio rerio*).[29]

Over the years, zebrafish have been increasingly used for studying the muscular dystrophies and are a powerful tool for drug discovery and therapeutic development.[33,34] Zebrafish models of DMD such as *sapje* and *sapje-like* recapitulate several features of the human disease. These include the absence of functional dystrophin and manifestation of severe dystrophic muscle phenotype. This phenotype is first observable on day 4 after fertilization by using a non-lethal optical technique based on the transparency of zebrafish larvae and the birefringence properties of zebrafish skeletal muscle.[35–38] Previous work from our laboratory took advantage of dystrophin-deficient zebrafish to perform phenotypic high-throughput small-molecule screening that would not be possible in mammalian systems, and we identified compounds that restore muscle integrity as seen by birefringence and improved survival.[39–41] Other laboratories have also been utilizing this assay to identify small molecules that may yield promising DMD therapies,[42–44] since some have been confirmed in DMD mouse models[41,43,45] or used in clinical trials.[46,47]

In the present study, we aimed to use the birefringence assay in dystrophin-deficient *sapje-like* zebrafish to identify new pathways that first reduce the manifestation of the DMD phenotype and then repress *pitpna* expression. We also incorporated additional relevant functional assessments to enhance the potential of novel drug discovery for DMD. We identified phosphodiesterase PDE10A inhibitors and validated that morpholino-mediated specific *pde10a* repression led to reduction in muscle pathology and improvement in locomotion, muscle, and vascular function as well as long-term survival in *sapje-like* zebrafish larvae. Moreover, PDE10A inhibition led to a reduction of *PITPNA* expression in the *sapje-like* zebrafish as well as DMD patient-derived myoblasts and holds promise for the development of a new therapeutic avenue.

RESULTS

PDE10A Inhibitors Reduce the Dystrophic Muscle Phenotype in Dystrophin Null Zebrafish Larvae

A short-term birefringence screening assay was performed to identify novel therapeutic candidates that limit the dystrophic muscle phenotype in dystrophin null *sapje-like* ($SL^{-/-}$) zebrafish. The non-selective PDE inhibitor aminophylline was used as positive control, which was discovered as a positive effector in a previous short-term birefringence screening assay in our laboratory and confirmed independently in dystrophin null zebrafish.[39,42,43,48] The design of our assay is presented in Figure 1A.

As previously described,[38] our assay confirmed that $SL^{-/-}$ larvae showed a characteristic "affected" patch-like pattern of birefringence with dark areas representing myofibrillar disorganization and muscle degeneration among bright areas of normal somatic muscle structures at 4 days post-fertilization (dpf) (Figure 1B). Whole-muscle birefringence intensity of individual $SL^{-/-}$ larvae was only 72% ($p < 0.05$) of the maximal birefringence seen in "unaffected" wild-type (WT) and unaffected heterozygous (Hets) siblings (Figure 1C), consistent with other *dmd* zebrafish lines.[49] Treatment with compound A and PF-02545920, two PDE10A small-molecule inhibitors, reduced the manifestation of the patch-like pattern of birefringence, especially in the dorsal muscle area (Figure 1B). The whole-muscle birefringence intensity of individual $SL^{-/-}$ larvae treated with compound A and PF-02545920 was significantly improved compared to control vehicle $SL^{-/-}$ larvae ($p < 0.05$) and represented ~84% of the maximal birefringence seen in WT/Hets siblings (Figure 1C). Interestingly, there was inter-fish variation in efficacy with a subtype of $SL^{-/-}$ larvae displaying birefringence intensity equivalent to that of their WT siblings (Figure 1C). In our assay, Mendelian genetics dictates 25% of the progeny to be dystrophin null and exhibit a dystrophic muscle phenotype seen by birefringence. Hence, deviation from this percentage was used to gauge the efficacy of the small molecules. The proportion of fish that manifested an abnormal muscle birefringence was significantly decreased when treated with compound A and PF-02545920 and represented ~19% and ~15% ($p < 0.05$) of the cohort, respectively (Figure 1D).

In previous studies, the PDE5 inhibitor sildenafil improved birefringence of dystrophin null zebrafish.[39,41] In the present study, we combined PDE10A inhibitors compound A or PF-02545920 and the PDE5 inhibitor sildenafil at different concentrations in *sapje-like* larvae (Figure S1). However, these combinations did not show any synergistic improvement of the muscle birefringence phenotype seen in our assay (Figure S1). It is noteworthy that PF-02545920 alone, from 0.15 to 0.5 μg/mL, and compound A alone at 2.5 μg/mL displayed the maximum muscle efficacy assessed by birefringence without affecting fish survival (Figure S1). The use of PF-02545920 at 0.15 μg/mL showed greater efficacy compared to the use of compound A at 2.5 μg/mL (Figure S1).

Taken together, these results clearly demonstrate that the use of PDE10A inhibitors compound A and PF-02545920 reduces the manifestation of the dystrophic muscle phenotype observed by birefringence in dystrophin null *sapje-like* zebrafish larvae.

The Use of *pde10a* Morpholino Reduces the Dystrophic Muscle Phenotype in Dystrophin Null Zebrafish Larvae

To validate PDE10A as a therapeutic target in *sapje-like* zebrafish, *pde10a* morpholino antisense oligonucleotide was injected in one-cell-stage embryos. Similar injections were carried out by using a standard control morpholino to demonstrate the specific effects of Pde10a inhibition. At 4 dpf, a muscle birefringence assay was performed, and extensive analysis of the phenotype was conducted to assess muscle and vascular function as well as survival of *sapje-like* zebrafish. The design of our morpholino study is presented in Figure 2A.

At 4 dpf, *pde10a* morphant zebrafish exhibited a 50% reduction of Pde10a protein level compared to non-injected siblings, while Pde10a protein expression was not altered in control morphant larvae

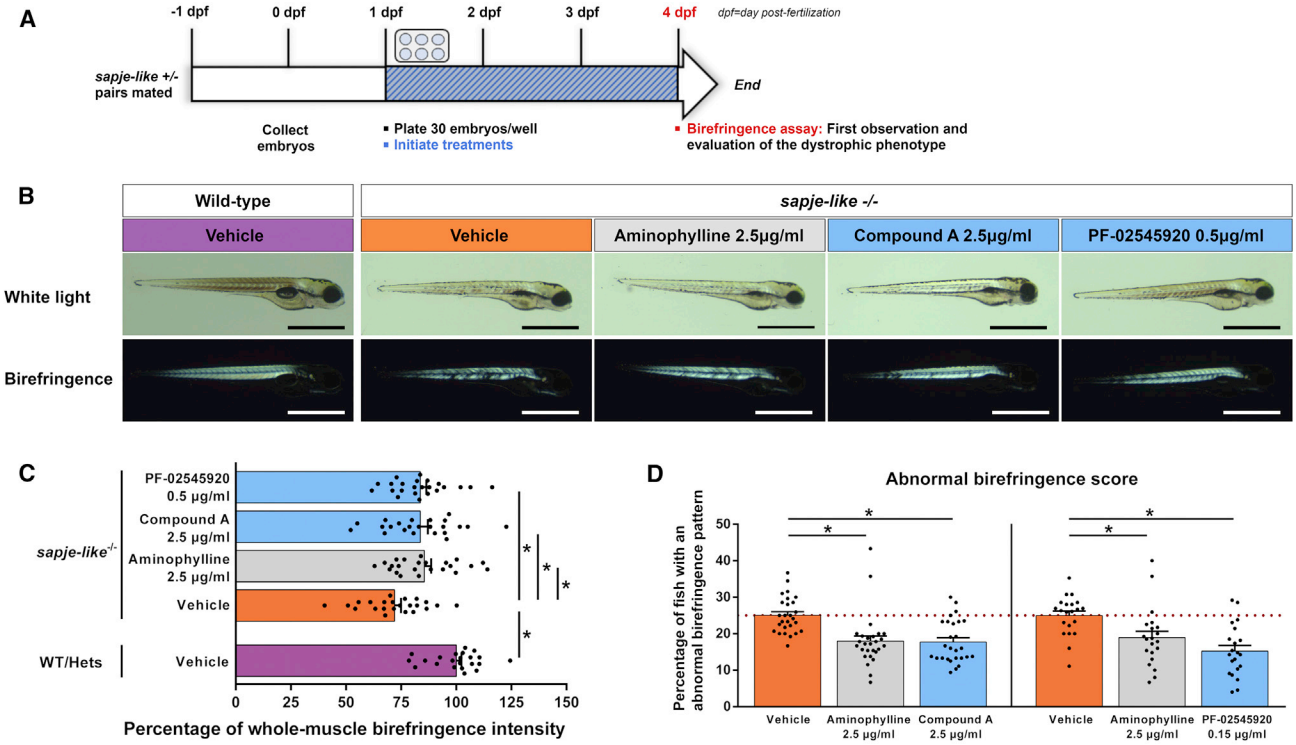

Figure 1. Short-Term Birefringence Screening Assay in Dystrophin-Deficient Zebrafish Identifies Phosphodiesterase 10A (PDE10A) Inhibitors That Reduce the Manifestation of the Dystrophic Muscle Phenotype

(A) Design of short-term birefringence screening assay in dystrophin-deficient *sapje-like* zebrafish: pairs of *sapje-like*$^{+/-}$ zebrafish were mated and treatments were applied to the progeny in six-well plates (30 embryos per well) from 1 day post-fertilization (dpf). At 4 dpf, a birefringence assay was performed. (B) White light and birefringence images of representative 4-dpf larvae treated with 0.1% DMSO (vehicle, control), 2.5 µg/mL aminophylline (positive control), 2.5 µg/mL compound A, or 0.5 µg/mL PF-02545920 (two PDE10A inhibitors from Pfizer). Scale bars represent 1 mm. (C) Dot plots showing percentage of whole-muscle birefringence intensity of 4-dpf larvae. The whole-muscle birefringence intensity was normalized to the area of measure and larvae were genotyped. At least 22 (n = 22) zebrafish per experimental treatment were analyzed in three (N = 3) independent experiments. Statistical differences between groups are presented as follows: *p < 0.05 (t test, ±SEM). WT, wild-type larvae; Hets, heterozygous sapje-like$^{+/-}$ larvae. (D) Dot plots showing percentage of 4-dpf larvae that display abnormal muscle birefringence pattern (named as abnormal birefringence score) in each well. Mendelian genetics dictates 25% of the progeny to be dystrophin null and exhibit the muscle dystrophic phenotype seen by birefringence (red dashed line). Experimental treatments were performed in triplicate wells in at least seven (N = 7) independent experiments. Statistical differences between groups are presented as follows: *p < 0.05 (t test, ±SEM).

(Figure 2B). On the same day, *pde10a* morphant $SL^{-/-}$ larvae exhibited a clear improvement in the skeletal muscle organization seen by birefringence and confirmed by phalloidin staining with fewer fiber detachments, unlike control morphant $SL^{-/-}$ larvae (Figure 2C). The whole-muscle birefringence intensity of individual *pde10a* morphant $SL^{-/-}$ was nearly restored to the WT/Hets sibling level (~95%, Figure 2D), while the whole-muscle birefringence intensity of control morphant $SL^{-/-}$ was not improved (~64%), compared to non-injected WT/Hets siblings (~65%, Figure 2D). Furthermore, the proportion of *pde10a* morphant larvae that manifested abnormal muscle birefringence was significantly decreased and represented about 18% of the cohort ($p < 0.05$), compared to ~25% in the non-injected sibling cohort (Figure 2E). Indeed, sequencing confirmed that around 6% of *pde10*a morphant zebrafish carried a dystrophin null genotype and escaped manifestation of abnormal muscle birefringence at 4 dpf (Figure S2A). In contrast, the proportion of control morphant zebrafish that manifested abnormal muscle birefringence was not reduced (Figure 2E), and no escaper larvae were identified in the cohort (Figure S2B).

These results clearly demonstrate that injection of a *pde10a* morpholino at the one-cell stage of development reduces manifestation of the dystrophic muscle phenotype seen by birefringence in *sapje-like* zebrafish larvae and mimics the use of PDE10A inhibitors.

Improvement in Long-Term Survival of *pde10a* Morphant Dystrophin Null Zebrafish Larvae

Following the birefringence assay, the survival of unaffected (WT, $SL^{+/-}$, and potential $SL^{-/-}$ escapers) and affected *sapje-like* siblings (that only contain $SL^{-/-}$ fish) was monitored for 30 days and is presented in Figure 3. The survival of affected *sapje-like* larvae started to decline around 10–12 dpf compared to unaffected siblings ($p < 0.05$) and reached 50% of survival at day 24. In contrast, the survival of *pde10a* morphant affected *SL* larvae was significantly improved

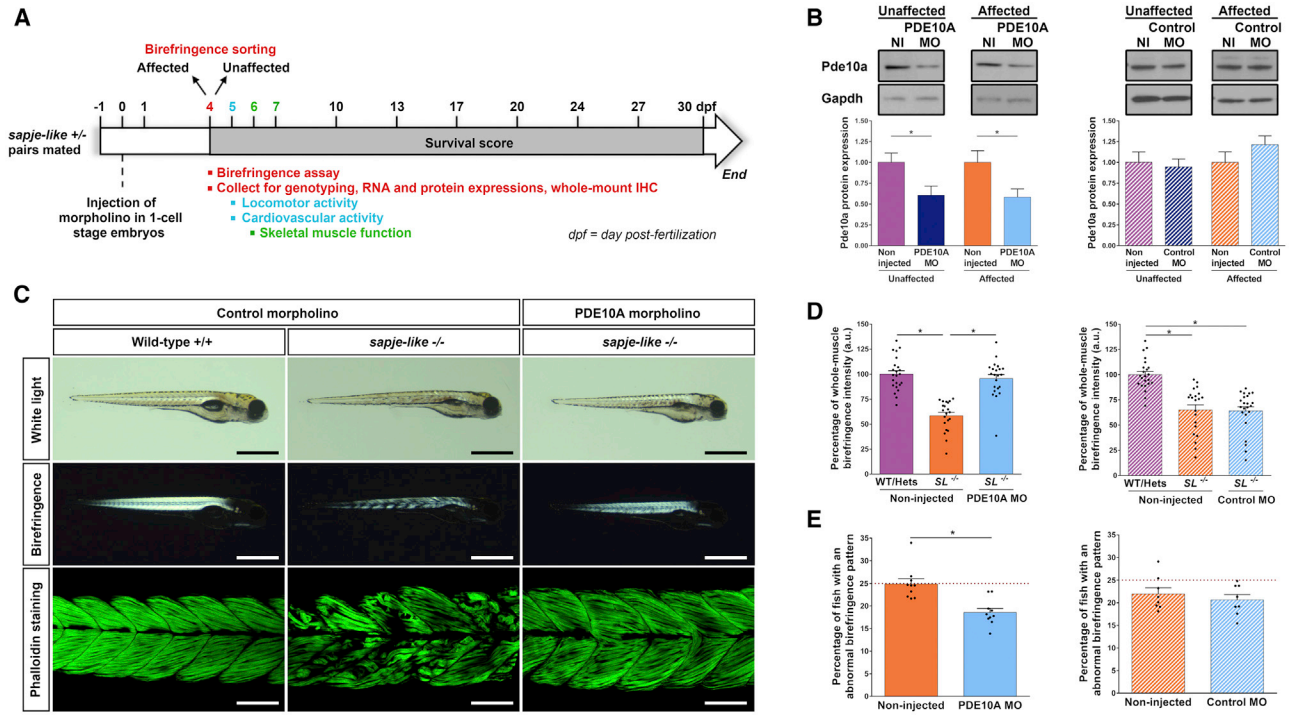

Figure 2. *pde10A* Morpholino Reduces the Manifestation of the Dystrophic Muscle Birefringence Phenotype in Dystrophin-Deficient Zebrafish

(A) Design of morpholino study: pairs of *sapje-like*$^{+/-}$ zebrafish were mated and *pde10A* morpholino or standard control morpholino (negative control) was injected in one-cell-stage progeny embryos. At 4 dpf, a birefringence assay was performed and unaffected (normal muscle birefringence phenotype) as well as affected larvae (abnormal muscle birefringence phenotype) were sorted to conduct genotyping or further analysis. In each experiment, morphant zebrafish (morpholino-injected larvae [MO]) were compared to non-injected siblings (non-injected larvae [NI]). (B) At 4 dpf, total proteins were extracted from 20 (n = 20) zebrafish per biological replicate and western blotting was performed. Upper panel: representative western blot images from Pde10a and Gapdh antibodies. Lower panel: bar graph showing Pde10a protein expression normalized to Gapdh. At least four (N = 4) independent experiments were performed. Statistical differences between groups are presented as follows: *$p < 0.05$ (t test, ±SEM). (C) White light, birefringence, and phalloidin staining images of representative 4-dpf larvae. Scale bars of white light and birefringence panels represent 1 mm. Scale bars of phalloidin staining panel represent 100 μm. (D) Dot plots showing percentage of whole-muscle birefringence intensity of 4-dpf larvae in *pde10a* morpholino experiments and control morpholino experiments. The muscle birefringence intensity was normalized to the respective area of measure, and larvae were genotyped. SL$^{-/-}$, dystrophin null sapje-like$^{-/-}$ larvae. Twenty-one to 23 (n = 21–23) zebrafish per group were analyzed in three (N = 3) independent experiments. Statistical differences between groups are presented as follows: *$p < 0.05$ (t test, ±SEM). (E) Dot plots showing percentage of 4-dpf larvae that display an abnormal muscle birefringence pattern (named as abnormal birefringence score) in *pde10a* morpholino experiments and control morpholino experiments. Mendelian genetics dictates 25% of the progeny to be dystrophin null and exhibit the muscle dystrophic phenotype seen by birefringence (red dashed line). Each dot represents the percentage of zebrafish that display an abnormal muscle birefringence pattern in a cohort (n = 200–300) of non-injected or morphant siblings. Eight to 10 (N = 8–10) independent experiments were performed per condition. Statistical differences between groups are presented as follows: *$p < 0.05$ (t test, ±SEM).

from day 12 to day 27 compared to non-injected affected siblings ($p < 0.05$), and it was similar to non-injected unaffected siblings by day 20 ($p > 0.05$, Figure 3A). The survival of control morphant affected *sapje-like* larvae was still impaired and followed the trend of non-injected affected sibling survival (Figure 3B).

Our results demonstrate that mildly affected *pde10a* morphant *sapje-like* larvae exhibit a longer lifespan similar to that of unaffected siblings at the early stage of life.

Improvement in Motor and Muscle Function of *pde10a* Morphant Dystrophin Null Zebrafish Larvae

Given the substantial correction of muscle phenotype and the longer lifespan in *pde10a* morphant *sapje-like* larvae, we hypothesized that motor function might be improved.

Motor function of dystrophin-deficient *sapje-like* larvae has never been documented. However, it is known that locomotor activity of juvenile zebrafish changes under different illumination conditions.[50–52] Using the DanioVision chamber (Noldus), we developed a light-dark locomotion assay in 48-well plates to analyze velocity (mm/min), distance traveled (mm), and maximum acceleration capacity (mm/s^2) of individual 5-dpf *sapje-like* larvae. The results are presented in Figure 4.

Upon the light condition, a pattern of gradually increased locomotor activity was monitored for 30 min in unaffected WT/Hets larvae, while this spontaneous locomotor activity was almost completely ablated in affected *SL*$^{-/-}$ larvae. Indeed, swimming velocity of *SL*$^{-/-}$ larvae was constantly reduced ($^{\#}p < 0.05$, Figure 4A) and the total distance traveled represented about 9% of normal assessed in WT/Hets

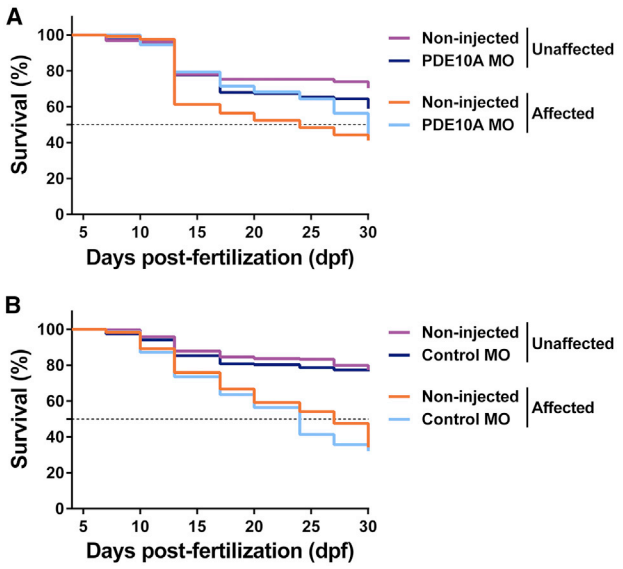

Figure 3. Lifespan Was Extended in *pde10a* Morphant Dystrophin-Deficient Zebrafish

Pairs of *sapje-like*$^{+/-}$ zebrafish were mated and *pde10a* morpholino or standard control morpholino (negative control) was injected in one-cell-stage progeny embryos. At 4 dpf, a birefringence assay was performed and unaffected larvae (normal muscle birefringence phenotype) as well as affected larvae (abnormal muscle birefringence phenotype) were sorted. (A and B) From 4 to 30 dpf, the survival of larvae in (A) *pde10a* morpholino experiments and (B) control morpholino experiments was evaluated and compared to non-injected siblings. One hundred thirty to 300 (n = 130–300) zebrafish per group were analyzed in at least three (N = 3) independent experiments. Statistical differences between groups were determined from a log-rank test ($p < 0.05$).

siblings ($p < 0.05$, Figure 4B). In contrast, the locomotion of *pde10a* morphant $SL^{-/-}$ fish was significantly improved since swimming velocity was constantly increased compared to non-injected $SL^{-/-}$ siblings (*$p < 0.05$, Figure 4A; Figure S3) and distance traveled was three times higher than in non-injected $SL^{-/-}$ siblings and represented about 27% of the total distance traveled by WT/Hets siblings ($p < 0.05$, Figure 4B; Figure S3). Furthermore, the maximum acceleration of $SL^{-/-}$ larvae was also reduced to 23% of capacity observed in WT/Hets siblings, while it was significantly improved in *pde10a* morphant $SL^{-/-}$ larvae and reached 38% of normal capacity (Figure 4D). Improvement of spontaneous locomotor activity upon the light condition was specific to *pde10a* morpholino injections since swimming velocity (Figure 4E), distance traveled (Figure 4F; Figure S3) and maximum acceleration capacity (Figure 4H) of control morphant $SL^{-/-}$ larvae were not improved compared to non-injected $SL^{-/-}$ siblings.

Following the light-to-dark transition, we were able to analyze swimming performance under more strenuous conditions since locomotor activity was sharply increased for about 10 min due to abrupt visual stimulus, and then gradually returned to baseline activity. During the 10-min acute response, swimming velocity (Figure 4A) and total distance traveled (Figure 4C) by $SL^{-/-}$ and WT/Hets siblings were similarly increased; however, the rise in maximum acceleration of $SL^{-/-}$ larvae was significantly impaired compared to WT/Hets siblings ($^{\#}p < 0.05$, Figure 4D). In contrast, the maximum acceleration of *pde10a* morphant $SL^{-/-}$ was improved, being similar to WT/Hets siblings for the first minute and was still significantly improved compared to non-injected $SL^{-/-}$ siblings after 5 min (*$p < 0.05$, Figure 4D); after 10 min, the maximum acceleration of *pde10a* morphant $SL^{-/-}$ reached the baseline level of non-injected $SL^{-/-}$ siblings (Figure 4D). Improvement of stimulated locomotor activity following the light-to-dark transition was specific to *pde10a* morpholino injections since maximum acceleration capacity of control morphant $SL^{-/-}$ larvae were similarly impaired compared to non-injected $SL^{-/-}$ siblings (Figure 4H). However, it is worth noting that the gradual return to baseline was impaired in the *pde10a* morphant WT/Hets larvae compared to non-injected WT/Hets siblings (Figures 4A, 4C, and 4D).

Altogether, these results clearly demonstrate that spontaneous and stimulated motor function of *pde10a* morphant *sapje-like*$^{-/-}$ was improved.

To assess whether the correction of muscle phenotype and the enhancement of motor function can be related to an improvement in muscle function, the force production of *sapje-like* trunk musculature was measured at 6–7 dpf. The results are presented in Figure 5. As previously described in dystrophin null *sapje* fish,[53] the twitch and tetanic forces of $SL^{-/-}$ fish were depressed to 63% of normal. In *pde10a* morphant $SL^{-/-}$, the twitch and tetanic forces were substantially increased by ~17% and reached about 73% of normal (Figures 5B and 5E). Injection of the control morpholino did not significantly change the force production compared to non-injected siblings (Figures 5C and 5F).

Besides the improvement of locomotor function, the results demonstrate that the muscle force production was also greater in *pde10a* morphant *sapje-like*$^{-/-}$ larvae and may contribute to the extended lifespan.

Improvement in Vascular Function of *pde10a* Morphant Dystrophin Null Zebrafish Larvae

As previously shown, death occurs at the early larval stage in dystrophin-deficient zebrafish, likely due to skeletal muscle defects and feeding failure.[33] However, cardiovascular dysfunction has never been studied in dystrophin-deficient zebrafish, which may be an additional cause of death as described in patients. At 5 dpf, $SL^{-/-}$ fish did not develop pericardial edema as seen in some zebrafish models of cardiac defect;[54] however, $SL^{-/-}$ larvae showed a decreased heart rate (113 ± 4 beats per minute [bpm]) compared to WT/Hets siblings (135 ± 4 bpm, Figure 6A). In contrast, the heart rate of *pde10a* morphant $SL^{-/-}$ was similar to the normal (134 ± 8 bpm, Figure 6A), while it was not improved in control morphant $SL^{-/-}$ (i.e., 118 ± 2 bpm, Figure 6B). Furthermore, the posterior cardinal vein of $SL^{-/-}$ appeared to be abnormal (Figure S4) and the blood flow was reduced to 68% of normal (Figure 6C). Representative videos of the blood flow from the posterior cardinal vein are presented in

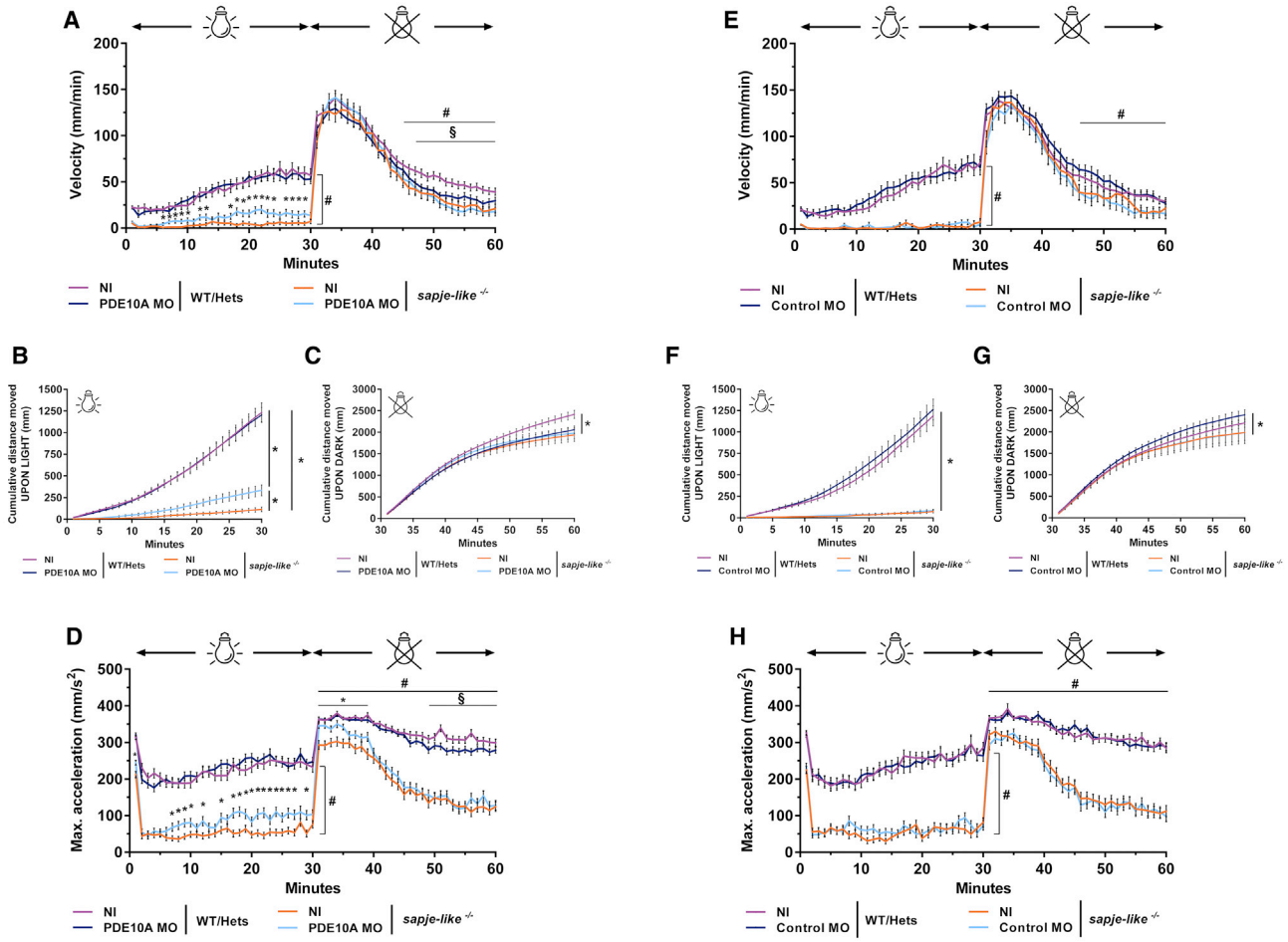

Figure 4. Improvement in Locomotion of *pde10a* Morphant Dystrophin-Deficient Zebrafish

Pairs of *sapje-like*$^{+/-}$ zebrafish were mated and *pde10a* morpholino or standard control morpholino (negative control) was injected in one-cell-stage progeny embryos. At 4 dpf, a birefringence assay was performed and unaffected larva (normal muscle birefringence phenotype) as well as affected larvae (abnormal muscle birefringence phenotype) were set in 48-well plates. At 5 dpf, following a dark period of acclimation, a light/dark locomotion assay was performed in the DanioVision observation chamber (Noldus) and data were generated from EthoVision XT tracking software (Noldus). In each experiment, morphant zebrafish were compared to non-injected siblings. At the end of the experiment, fish were collected and genotyped. (A–D) *pde10a* morpholino experiments. (E–H) Standard control morpholino experiments. (A and E) Graphs show swimming velocity (mm/min) for the entire assay. # indicates statistical differences between NI $SL^{-/-}$ and NI WT/Hets larvae; asterisk (*) indicates statistical differences between NI $SL^{-/-}$ and *pde10a* morphant $SL^{-/-}$ larvae; § indicates statistical differences between NI WT/Hets and *pde10a* morphant WT/Hets ($p < 0.05$, t test, ±SEM). (B and F) Graphs show cumulative distance traveled (mm) for 30-min light period. Statistical differences between groups are presented as follows: *$p < 0.05$ (t test, ±SEM). (C and G) Graphs show cumulative distance traveled (mm) for 30-min dark period following light-to-dark transition. Statistical differences between groups are presented as follows: *$p < 0.05$ (t test, ±SEM). (D and H) Graphs show maximum acceleration capacity (mm/s^2) for the entire assay. # indicates statistical differences between NI $SL^{-/-}$ and NI WT/Hets larvae; asterisk (*) indicates statistical differences between NI $SL^{-/-}$ and *pde10a* morphant $SL^{-/-}$ larvae; § indicates statistical differences between NI WT/Hets and *pde10a* morphant WT/Hets ($p < 0.05$, t test, ±SEM). From 90 to 230 (n = 90–230) zebrafish were analyzed per condition within at least four (N = 4) independent experiments.

Videos S1, S2, S3, and S4 (related to Figure 6). In contrast, the posterior cardinal vein blood flow of *pde10a* morphant $SL^{-/-}$ was improved and represented 90% of normal (Figure 6C), while it was still impaired in control morphant $SL^{-/-}$ (Figure 6D).

These results show that dystrophin-deficient *sapje-like* fish might display an early impairment of vascular function that is restored by knockdown of *pde10a* and might contribute to the extended lifespan of *sapje-like* fish.

PDE10A Inhibition Reduced *PITPNA* Expression in Dystrophin Null Zebrafish Larvae and DMD Patient-Derived Myoblasts

Based on the GRMD *escaper* dog story,[29] the basis of our study was to identify small-molecule targets that, when inhibited, improved the muscle birefringence and repressed the genetic modifier *pitpna*.

At 4 dpf, *pde10a* morphant $SL^{-/-}$ exhibited an ~50% reduction of *pitpna* transcript (Figure 7A) and protein level (Figure 7B), while control morphant larvae did not exhibit any alteration of *pitpna*

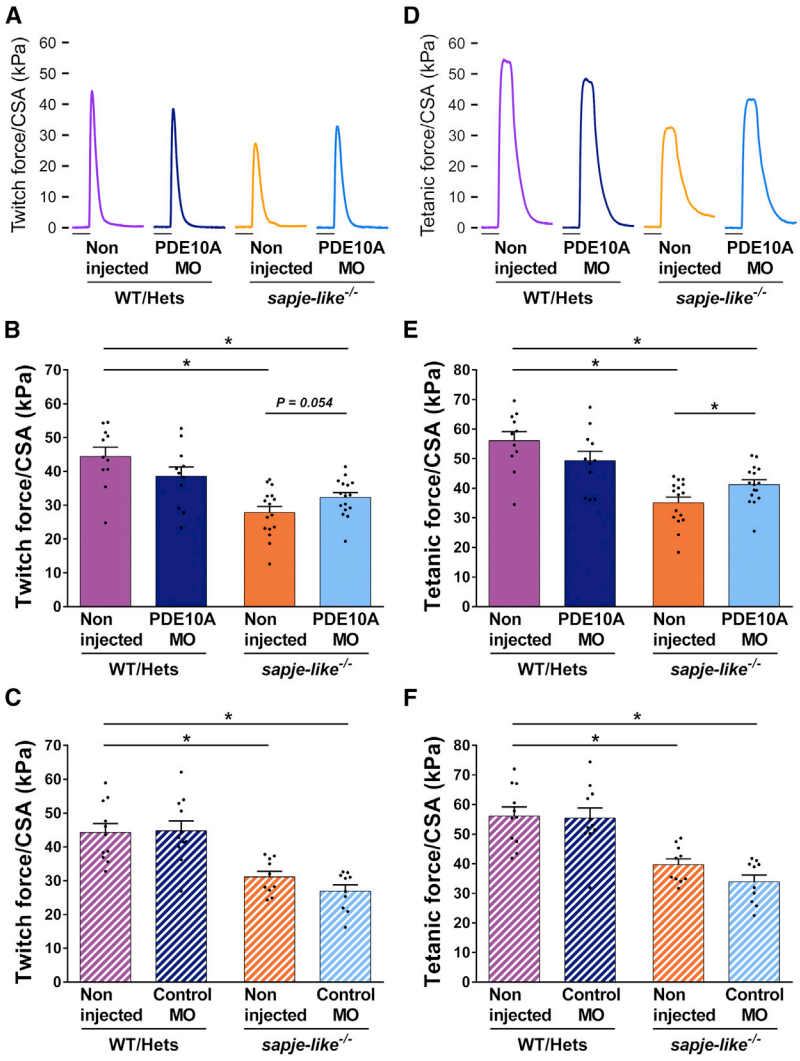

Figure 5. Increase in Specific Force Produced by *pde10a* Morphant Dystrophin-Deficient Zebrafish

Pairs of *sapje-like*$^{+/-}$ zebrafish were mated and *pde10a* morpholino or standard control morpholino (negative control) was injected in one-cell-stage progeny embryos. At 4 dpf, a birefringence assay was performed and unaffected larvae (normal muscle birefringence phenotype) as well as affected larvae (abnormal muscle birefringence phenotype) were sorted. At 6–7 dpf, twitch and tetanic force were measured in the tails and normalized to the cross-section area (CSA). In each experiment, morphant zebrafish were compared to non-injected siblings. At the end of the experiment, fish were collected and genotyped. (A and D) Representative twitch (A) and tetanic force signal (D) are shown. Scale bars represent 50 ms. (B and C) Dot plots show twitch force (kPa) in (B) *pde10a* morpholino experiments and (C) control morpholino experiments. (E and F) Dot plots showing tetanic force (kPa) in (E) *pde10a* morpholino experiments and (F) control morpholino experiments. Eleven to 16 (n = 11–16) zebrafish per group were analyzed within at least three (N = 3) independent experiments. Statistical differences between groups are presented as follows: *p < 0.05 (t test, ±SEM).

expression (Figures 7A and 7B). In the baseline condition (non-injected), affected *SL*$^{-/-}$ fish exhibited an increase of *pitpna* mRNA level (Figure S5A), similar to the observation in GRMD dogs.[29] In the mildly affected *pde10a* morphant *SL*$^{-/-}$, *pitpna* expression was decreased and restored to baseline level of unaffected WT/Hets siblings (Figure S5A); a similar change in *Pitpna* expression was observed in the notable GRMD *escaper* dogs.[29] Interestingly, *SL*$^{-/-}$ larvae treated with PDE10A inhibitor PF-02545920 also exhibited decreased *pitpna* transcript at 4 dpf (Figure S5B).

Based on our findings, we aimed to assess the efficacy of PDE10A inhibition in primary cultures of DMD patient cells. PDE10A inhibitor PF-02545920 was applied to primary cultures of CD56^{+} DMD patient-derived myoblasts and myotubes. Treatment of DMD patient-derived myoblasts with 25 μM PF-02545920 for 24 h led to a reproducible and significant reduction (~30%–40%) of *PITPNA* mRNA (Figure 7C) and protein expression (Figure 7D). In myotubes, treatment with 25 μM PF-02545920 at day 6 of differentiation for 24 h led to similar decrease of *PITPNA* mRNA expression (Figure 7C) while it did not influence PITPNA protein expression (Figure 7D).

These results demonstrate that PDE10A is a potential modulator of *PITPNA* expression in the *sapje-like* zebrafish and DMD patient-derived myogenic cells.

DISCUSSION

In the present study, we identified PDE10A inhibitors that reduce the dystrophic muscle phenotype by using our birefringence screening assay in dystrophin-deficient *sapje-like* zebrafish larvae. This pathway was then validated by using a morpholino antisense oligonucleotide that led to specific repression of *pde10a* and to similar restoration of muscle integrity. In addition to our phenotypic assay, we designed a workflow of different functional assessments that enhanced the potential for the prospective discovery of DMD therapeutics. We have built on previous behavioral studies and assessed the locomotion of *sapje-like* larvae combined with the measure of muscle function. We showed that specific repression of *pde10a* improved motor and muscle function, as well as vascular function and long-term survival, in *sapje-like* larvae. These different points are discussed below.

PDEs are recognized for being essential regulators of the cellular content and subcellular compartmentalization of cyclic nucleotides by catalyzing the degradation of 3′,5′-cyclic AMP (cAMP) and 3′,5′-cyclic GMP (cGMP), which are used as second messengers for a wide range of signaling pathways and physiological processes.[55,56] To date, 11 families of PDEs have been identified that have unique

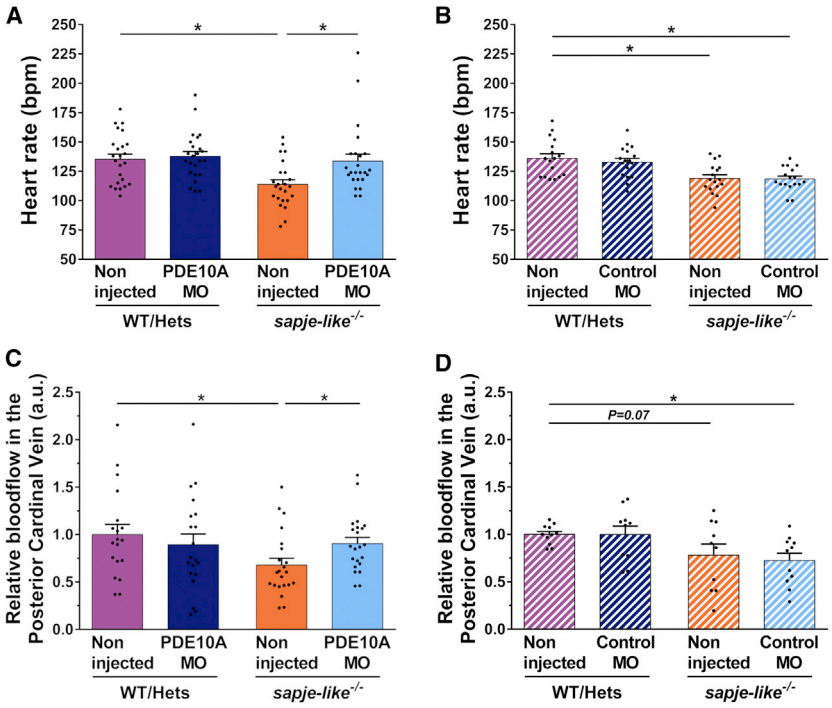

Figure 6. Improvement in Cardiovascular Activity of *pde10a* Morphant Dystrophin-Deficient Zebrafish

Pairs of *sapje-like*$^{+/-}$ zebrafish were mated and *pde10a* morpholino or standard control morpholino (negative control) was injected in one-cell-stage progeny embryos. At 4 dpf, a birefringence assay was performed and unaffected larva (normal muscle birefringence phenotype) as well as affected larvae (abnormal muscle birefringence phenotype) were sorted. At 5 dpf, anesthetized larvae were recorded for at least 30 s under a microscope. In each experiment, morphant zebrafish were compared to non-injected siblings. At the end of the experiment, fish were collected and genotyped. (A and B) Dot plots show the heart rate (beats per minute [bpm]) of 5-dpf larvae in (A) *pde10a* morpholino experiments and (B) control morpholino experiments. Seventeen to 24 (n = 17–24) zebrafish were analyzed within at least three (N = 3) independent experiments. Statistical differences between groups are presented as follows: *p < 0.05 (t test, ±SEM). (C and D) Dot plots show blood flow (arbitrary units [a.u.]) of posterior cardinal vein in (C) *pde10a* morpholino experiments and (D) control morpholino experiments. Blood flow was measured by using DanioScope software (Noldus). Ten to 22 (n = 10–22) zebrafish were analyzed within at least three (N = 3) independent experiments. Statistical differences between groups are presented as follows: *p < 0.05 (t test, ±SEM).

substrate sensitivity, tissue distribution, and subcellular localization. Therefore, PDE dysfunctions are associated with a multitude of pathophysiological states and provide the basis for considering PDEs as therapeutic targets.[56] Initial studies showed that total PDE activity was exacerbated in young (but not old) dystrophin-deficient *mdx* hind leg muscle (5–8 weeks).[57,58] Human studies also showed that PDE activity was elevated in quadriceps of young patients with DMD (4–6 years).[59] In our present study, we showed that inhibition of Pde10a improved the birefringence pattern in 4-dpf *sapje-like* larvae, and it is an indicator for the reduction of muscle degeneration, as previously described.[38] Our finding adds PDE10A inhibitors to the other PDE inhibitors, that is, PDE4 and PDE5, previously identified by Kawahara et al.,[39] using the birefringence screening assay in dystrophin-deficient zebrafish, as potential modulators of the DMD muscle phenotype. PDE4 inhibitors affect the cAMP-protein kinase A (PKA) pathway while PDE5 inhibitors modulate the nitric oxide (NO)- soluble Guanylate Cyclase (sGC)-cGMP-Protein Kinase G (PKG) pathway that are both attenuated in *mdx* mice.[60,61] Chronic treatment with PDE4 inhibitor piclamilast or PDE5 inhibitor sildenafil showed a potent anti-fibrotic and anti-inflammatory effect in the gastrocnemius muscle of *mdx* mice associated with a reduction of serum creatine kinase (CK), while the combination of both inhibitors showed a synergistic effect.[62] PDE10A is a dual-substrate PDE that hydrolyzes both cAMP and cGMP. In our birefringence assay, the combination of PDE5 and PDE10A inhibitors did not show any synergistic effect. However, we did not assess the anti-fibrotic and anti-inflammatory aspects. PDE10A is known to be expressed in skeletal and cardiac muscle as well as in vascular tissues, among others,[62–65] and the tissue distribution has to be considered in the dystrophic context for further phenotypic characterization in order to differentiate the action of PDE10A from the other PDEs.

In addition to our phenotypic assay, we incorporated different functional assays that have never been documented in *sapje-like* zebrafish. Zebrafish larvae show a plethora of swimming behaviors and are sensitive to a variety of stimulus modalities.[50–52] The light-dark locomotor assay creates a pattern of stress-induced movements in the dark for a short period of time, followed by a resting state in the light, and it has been used in high-throughput screening of various neuroactive drugs.[50–52] Absence of dystrophin is known to reduce locomotion in *sapje* larvae;[29,35] however, it has never been analyzed and quantified in dystrophin-deficient *sapje-like*. Using an automatic system (DanioVision, Noldus), the locomotor activity between *sapje-like* and WT siblings at 5 dpf was clearly distinct. In the light, the locomotor activity of *sapje-like* larvae was almost absent while the distance traveled by WT siblings was 10-fold higher and the velocity as well as the maximum acceleration were increased by 5-fold. This difference was then reduced in the dark. Thus, this assay could be widely used to assess efficacy of therapeutics in motor function of dystrophin-deficient *sapje-like* larvae.

In our study, morpholino-mediated *pde10a* repression partially (and significantly) restored locomotor activity in *sapje-like* larvae. Because PDE10A is also highly expressed in the striatum that controls motor, emotional, and cognitive function,[56] the influence of the central system cannot be excluded in our assay. Indeed, we noticed that *pde10a*

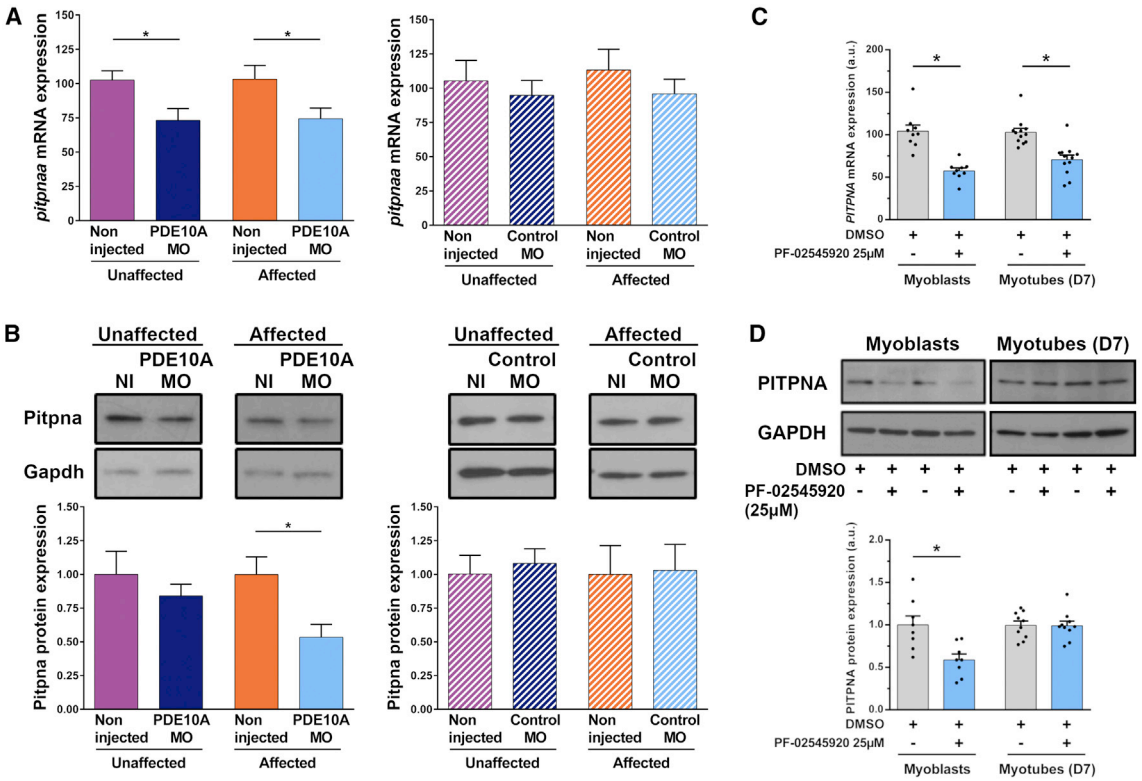

Figure 7. PDE10A Inhibition Leads to Reduction of *PITPNA* Expression in Dystrophin-Deficient Zebrafish and DMD Patient-Derived Myoblasts

Pairs of *sapje-like*$^{+/-}$ zebrafish were mated and *pde10a* morpholino or standard control morpholino (negative control) was injected in one-cell-stage progeny embryos. At 4 dpf, a birefringence assay was performed and unaffected (normal muscle birefringence phenotype) as well as affected larvae (abnormal muscle birefringence phenotype) were collected. In each experiment, morphant zebrafish were compared to non-injected siblings. (A) Total mRNA was extracted from 10 (n = 10) zebrafish per biological replicate and TaqMan qRT-PCR was performed. Bar graphs show *pitpna* mRNA expression normalized to *hprt1*. In each experiment, the replicate was run three times and at least five (N = 5) independent experiments were performed. Statistical differences between groups are presented as follows: *$p < 0.05$ (t test, ±SEM). (B) Total proteins were extracted from 20 (n = 20) zebrafish per biological replicate and western blotting was performed. Upper panel: representative western blot images from Pitpna and Gapdh antibodies. Lower panel: bar graph showing Pitpna protein expression normalized to Gapdh. At least four (N = 4) independent experiments were performed. Statistical differences between groups are presented as follows: *$p < 0.05$ (t test, ±SEM). (C) In a primary culture of CD56-positive myoblasts and myotubes (at day 6 of differentiation) from DMD patients, 25 μM PDE10A inhibitor PF-02545920 or 0.25% DMSO (control) was applied for 24 h. Total mRNA was extracted and TaqMan qRT-PCR was performed. Bar graph shows PITPNA mRNA expression normalized to GAPDH. (D) Total proteins were extracted and western blotting was performed. Upper panel: representative western blot images with PITPNA and GAPDH antibodies. Lower panel: bar graph showing PITPNA protein expression normalized to GAPDH. In each experiment, two DMD patient cell lines were used, and replicates were run three times in at least three (N = 3) independent experiments. Statistical differences between groups are presented as follows: *$p < 0.05$ (t test, ±SEM).

repression might not be beneficial for motor function in WT fish, since locomotor activity was slightly impaired following the light-to-dark stimulus. Thus, direct measures of muscle function must be combined with this behavioral assay. Additional experiments showed that the enhancement of locomotor activity in *pde10a* morphant *sapje-like* larvae was associated with a 17% increase in specific force ($p < 0.05$) in the tail and muscle trunk. Our data were generated at 6–7 dpf, and greater improvement might be expected at an earlier stage of development (i.e., 4 dpf) since the morpholino dilutes through mitotic activity over time. A similar range of efficacy was reported in *mdx* mice diaphragm treated with sildenafil that exhibited a 15% increase in specific force.[45] Indeed, the use of sildenafil, or another PDE5 inhibitor, tadalafil, showed promising results to slow the progression of ambulatory, respiratory, and cardiac dysfunctions in *mdx* and GRMD dogs,[45,66–69] while functional sympatholysis was restored and the decline of motor performance was delayed in upper limbs of patients.[47,70] However, sildenafil and tadalafil did not improve cardiac and ambulatory functions of patients, respectively.[46,70] Failure of PDE5 inhibition to restore some function in patients might be due to the administration of treatment after evident decline of function; therefore, a prophylactic use (before 7 years of age) might be recommended as seen in DMD animal models. In our study, PDE10A morpholino or small-molecule inhibitors were applied before the onset of muscle degeneration in *sapje-like* larvae. Although the benefits of prophylactic application of PDE10A inhibitors is important to demonstrate, future studies are needed to determine whether application after onset of pathology will also induce similar benefits.

Altogether, our data raise the intriguing question of how some *pde10a* morphant dystrophin-deficient larvae that manifested not full but partial improvement of muscle phenotype and function can exhibit a similar survival rate to WT larvae by 17 dpf. Besides alteration of vascular function, cardiomyopathy is emerging as the leading cause of death among patients with DMD,[13] and it has been little studied in dystrophin-deficient zebrafish. Clear alteration of vasculogenesis has been documented in *sapje* larvae,[41] which is consistent with our observation in *sapje-like* in which the posterior cardinal vein was not clearly defined and the blood flow was impaired, and reduction of *pde10a* expression was associated with restoration of blood flow. Due to technical limitations, we were not able to record blood circulation in non-anesthetized larvae, and we were not able to assess the microvasculature that surrounds muscles. Further characterizations are necessary to determine whether *sapje-like* larvae represents a pertinent model to study vascular function in the DMD context given that patients with DMD typically manifest alteration of intramuscular blood flow after exercise.[47,71] Furthermore, we also characterized a decrease of the heart rate in *sapje-like* larvae that was restored when *pde10a* expression was reduced. Cardiac defects typically manifest as pericardial edema in zebrafish larvae,[54] as seen in the zebrafish model of LGMD2I.[72] In our study, neither non-injected nor morphant *sapje-like* larvae manifested pericardial edema at 5 dpf; therefore, changes in blood circulation and heart rate are not likely due to a cardiac defect, but rather a faulty vasculature system. However, a late development of cardiac failure cannot be excluded since patients with DMD develop cardiomyopathy in the second decade and exhibit alteration of heart rate. Further experiments need to be done since a recent study showed that PDE10A inhibition can reduce fibrosis and restore cardiac function in mouse models of cardiac diseases.[65] Altogether, our data suggest that repression of *pde10a* also has a protective effect on vasculature function and may be one of the mechanisms that extend the lifespan of dystrophin-deficient *sapje-like* larvae.

Overall, our study presents additional evidence that the dystrophin-deficient *sapje-like* zebrafish is a relevant model in order to identify new targets that influence different aspects of DMD pathology, and thereby an important complement to the more established mammalian models. Our experiments indicate that not do only dystrophin-deficient *sapje-like* zebrafish replicate the skeletal muscle defects of DMD, but they may also model some aspects of the cardiovascular pathology associated with dystrophin deficiency. However, phenotypic screening with small molecules designed to modulate human target proteins introduces the complexity of species translation and associated risks of screen failure and off-target effects, resulting in false positives. In our study, PF-02545920 induced toxicity above 0.3 μg/mL and did not improve long-term survival in *sapje-like* larvae, while PF-02545920 at 25 μM did not induce any toxic effect in primary human cell cultures (data not shown). Therefore, in zebrafish, target validation studies must be considered by evaluating zebrafish-specific morpholinos for target-specific knockdown effects similar to those achieved by the small molecules. The morpholino-induced effect should also be confirmed by using a negative standard control morpholino in the same study.[73]

The basis of our study was also to identify small molecules and validate pathways that repress the genetic modifier *pitpna* in *sapje-like* zebrafish. *Pitpna* has been identified as the exclusive gene differentially expressed between severe GRMD dogs and *escaper* GRMD dogs that carry a variant in the *Jagged1* promoter.[28,29] The protective effect of *pitpna* repression was confirmed by injection of *pitpna* morpholino in DMD *sapje* zebrafish that led to a restoration of the muscle phenotype, a greater swimming ability, and to a prolonged lifespan.[29] PITPNA is an important modulator of lipid signaling and membrane trafficking,[74–76] and we have previously shown that repression of *PITPNA* also led to reduction of PTEN levels and increase of phosphorylated AKT (pAKT) in the DMD context.[29] Induction of AKT signaling is known to play a significant role in muscle growth, vascularization, and metabolism, and to block the dystrophic pathogenesis.[77–83] In our study, reduction of *pde10a* expression in *sapje-like* led to *pitpna* repression, while the transcript level of *jagged1* was not changed (data not shown). In DMD patient-derived myoblasts, the selective PDE10A inhibitor PF-02545920 led to similar repression of *PITPNA*. However, the repression of *PITPNA* was seen only at the transcript level during later stages of differentiation. We did not test PDE10A inhibitors at earlier stages of differentiation nor after longer treatment times. Moreover, we do not exclude the possibility that PDE10A inhibition-mediated reduction of *pitpna* expression in *sapje-like* zebrafish might achieve its effect through other cell types in muscle. Thus, further cell-based experiments must also consider the efficacy of PDE10A inhibitors in other cell types from DMD patients.

In conclusion, PDE10A inhibition presents several reasons to be further studied as a potential DMD therapeutic. (1) PDE10A inhibitors are known to be safe since PF-02545920 has already been used in several clinical trials for treating schizophrenia and Huntington's disease,[56] and they have been described as a potential candidate for treating obesity and diabetes,[63] as well as colorectal cancer.[84] (2) Moreover, the level of *PITPNA* repression was similar to that described in the *escaper* dogs (30%–40% repression) and might reflect the safe range of efficacy since complete loss of Pitpna in mice leads to severe pathologies and premature death.[85] (3) Interestingly, the use of a PDE5 morpholino and the PDE5 inhibitor sildenafil in *sapje-like* larvae and in primary human muscle cell culture did not decrease the expression of *PITPNA* (data not shown), so it is likely that PDE5 and PDE10A regulate distinct pathways. (4) PDE10A inhibition led to partial (but still significant) reduction in muscle pathology, and improvement in motor, muscle, and vascular function in *sapje-like* larvae. In general, animal models or DMD patients who express genetic modifiers for DMD present with a delay in the onset of the disease or a mild phenotype in the best case. Thus, an intervention that aims to modulate a genetic modifier would not likely completely reduce disease outcomes or restore function per se. However, there is still precedence to pursue pharmacological therapies targeting genetic modifiers for DMD. Indeed, modest benefit can be particularly important for patient quality of life while there is no available cure. Moreover, effective treatment for DMD is likely to require a combination of therapies that complement both the primary defect and

its different secondary consequences.[86] Finally, the modulation of genetic modifiers aims to improve function regardless of patients' genetic mutations, so that it can be of interest for all patients. (5) We are aware that further studies are necessary to determine whether *pitpna* repression per se is driving the reduction of disease outcomes mediated by PDE10A inhibition in *sapje-like* larvae, and we do not exclude that additional pathways may be involved. However, our study suggests that PDE10A inhibition-mediated repression of *pitpna* might be beneficial in *sapje-like* zebrafish and supports a new indication for PDE10A inhibitors as potential DMD therapeutics to be further investigated in a mouse model of DMD.

MATERIALS AND METHODS

Zebrafish

Dystrophin-deficient *sapje-like* zebrafish (sap^{cl100}) were housed in the Boston Children's Hospital Aquatics Facility (environmental and housing conditions are available at https://dx.doi.org/10.17504/protocols.io.bb2iiqce). The study was carried out in strict accordance with the Institutional Animal Care and Use Committee (protocol #18-08-3749R).

Genotyping of *sapje-like* Zebrafish

Genomic DNA was extracted and used as a PCR template with the following primer set: forward, 5′-TCTGAGTCAGCTGACCACA GCC-3′ and reverse, 5′-ATGTGCCTGACATCAACATGTGG-3′. Sanger sequencing was performed in the Boston Children's Hospital Intellectual and Developmental Disabilities Research Center Molecular Genetics Core to identify the G-to-A mutation in the donor splice junction of dystrophin exon 62 that leads to a premature stop codon and absence of functional muscle dystrophin in $sapje\text{-}like^{-/-}$ zebrafish as previously described.[38]

Short-Term Birefringence Assay for Small-Molecule Screening

The design of the short-term birefringence assay is presented in Figure 1A. Pairs of Hets $sapje\text{-}like^{+/-}$ zebrafish were mated, and progeny embryos were collected and maintained at 28.5°C. On day 1 after fertilization, embryos were dechorionated and placed in six-well plates with 30 embryos/well. Each well contained an experimental treatment that was initiated on 1 dpf and renewed on 2 dpf. In the present study, PDE10A inhibitors (compound A, referenced as compound 26,[87] and PF-02545920,[88] both from Pfizer) and a PDE5 inhibitor (#PZ0003, sildenafil citrate salt, Sigma-Aldrich) in the presence of 0.1% DMSO (#D5879, Sigma-Aldrich) in E2 water were used as experimental treatments. Control conditions of 0.1% DMSO in E2 water and positive control conditions of 2.5 µg/mL aminophylline (#A1755, Sigma-Aldrich) in the presence of 0.1% DMSO in E2 water were also applied in each experiment. On 4 dpf, the dystrophic muscle phenotype was evaluated by using a birefringence assay that involves passing polarized light through the transparent zebrafish under the microscope. Briefly, larvae were anesthetized with 0.02% tricaine (MS-222, Sigma-Aldrich) and aligned between two polarizing filters on a Zeiss Discovery V8 stereomicroscope. One filter was rotated to visualize the maximum birefringence illumination, and larvae were imaged under similar light exposure by using ZEN software (Zeiss). Dystrophin null $sapje\text{-}like^{-/-}$ larvae show a characteristic patch-like pattern of birefringence (Figure 1B), with dark areas representing myofibrillar disorganization and muscle degeneration among bright areas of normal somatic muscle structures as previously described.[38] Mendelian genetics dictates 25% of the progeny to be homozygous dystrophin null and exhibit this dystrophic muscle birefringence phenotype. Deviations from this percent as an abnormal birefringence score was used to gauge muscle efficacy of the small molecules as previously described.[39,40] Each well corresponded to a biological replicate (n) in which the percent of larvae that manifested an abnormal birefringence pattern has been scored. At least three (n = 3) replicates have been performed in each independent experiment (N). Whole-muscle birefringence intensity normalized to the selected area was also quantified by using ImageJ as previously described,[49,89] and it was used to gauge muscle efficacy of the small molecules in individual *sapje-like* larva. At least 22 (n = 22) larvae per experimental treatment were analyzed within three (N = 3) independent experiments.

Confirmation of Candidate Small Molecules by Using Morpholino Antisense Oligonucleotides in *sapje-like* Zebrafish

Pairs of Hets $sapje\text{-}like^{+/-}$ zebrafish were mated and *pde10A* translation blocking morpholino (5′-TCCATGTCTGACCGCCAGCGAG TAG-3′, Gene Tools) was injected in one-cell-stage embryo progeny. Specificity of *pde10A* morpholino injections was evaluated by performing similar injection procedure with a negative standard control morpholino (5′-CCTCTTACCTCAGTTACAATTTATA-3′, Gene Tools) widely used in previous studies. Approximately 200–300 embryos were injected in each independent experiment (N). On 4 dpf, the dystrophic muscle phenotype was evaluated by birefringence assay as described above, and the abnormal birefringence score was determined in at least eight (N = 8) independent experiments. The whole-muscle birefringence intensity was also determined in at least 21 (n = 21) larvae per group within three (N = 3) independent experiments. At the end of the birefringence assay, larvae were genotyped as described above.

In other independent experiments, unaffected larvae with a normal birefringence pattern and affected larvae with an abnormal birefringence pattern were sorted and went through an extensive study in which muscle and cardiovascular function as well as lifespan were evaluated as described in Figure 2A. Procedure details are presented below.

Whole-Mount Immunohistochemistry Staining of *sapje-like* Larvae

Zebrafish embryos were fixed overnight in 4% paraformaldehyde (PFA) and then washed twice in PBS and 1% PBS-Tween 20 for 10 min, respectively. Embryos were then permeabilized at the room temperature for 1 h in 2% PBS-Triton X-100 on the slow shaking rotor. Next, embryos were washed twice with 1% PBS-Tween 20 for 5 min and blocked for 1 h in 5% goat serum (Sigma, G9023) in 1% PBS-Tween 20. Phalloidin antibody (Alexa Fluor 488, A12379,

Invitrogen) was added to the blocking solution (1:20) and to the fixed and blocked embryos and shacked further overnight at 4°C in the dark. The day after, embryos were washed twice with 1% PBS-Tween 20 for 15 min, stained with Hoechst (1:1,000) for 10 min, washed again with 1% PBS-Tween 20, and mounted in 3% methylcellulose (Sigma, M0387-100G). Phalloidin whole-mount staining was imaged by using a Zeiss LSM 700 laser scanning confocal microscope and ZEN software.

Long-Term Survival Assay

Following morpholino injections and a birefringence assay, the long-term survival of affected and unaffected zebrafish was assessed from 4 to 30 dpf. Mortality was counted every other day and statistical differences between groups were determined as follows: $p < 0.05$ using the log-rank test. At least 130 (n = 130) larvae per group were used on 4 dpf within three (N = 3) independent experiments.

Procedures for Zebrafish Protein Expression Analysis

Total protein content of 20 or more 4-dpf affected and unaffected larvae were separately extracted in a lysing Matrix D tube (MP Biomedicals) containing cold M-PER mammalian protein extraction reagent (Thermo Scientific) with anti-proteases (cOmplete, mini, EDTA-free, Roche) and anti-phosphatases (PhosSTOP, Sigma-Aldrich). Protein extracts were homogenized for 1 h at 4°C and centrifuged at 13,500 rpm for 30 min at 4°C. Protein concentration from the supernatant was determined using a Pierce bicinchoninic acid (BCA) protein assay kit (Thermo Scientific). In order to perform SDS-PAGE, protein contents were denatured in Novex Tris-glycine SDS buffer (Invitrogen) containing 50 mM dithiothreitol (NuPAGE reducing agent, Invitrogen) and boiled for 8 min at 95°C. Protein samples were separated on Novex 4%–20% Tris-glycine mini gels (Invitrogen) and transferred to a 0.2-μm polyvinylidene fluoride (PVDF) membrane (Invitrogen). Membranes were blocked in 5% non-fat dry milk in TBST (Tris-buffered saline [Boston BioProducts] with 0.05% Tween 20). Membranes were then blotted with primary antibodies (anti-Pde10a, 1:2,000, ab151454, Abcam; anti-Pitpna, 1:1,000, ab180234, Abcam; anti-Gapdh, 1:1,000, sc-47724, Santa Cruz Biotechnology) in blocking solution overnight at 4°C. After three 10-min washes in TBST, membranes were probed with secondary antibodies (immunoglobulin G [IgG], horseradish peroxidase [HRP]-linked, 7076S or 7074S, Cell Signaling Technology) in blocking solution for 2 h at room temperature, and finally extensively washed in TBST. Chemiluminescence detection was captured using Pierce enhanced chemiluminescence (ECL) western blotting substrate (Thermo Scientific) and X-ray film (Genesee Scientific). Protein signal intensities were analyzed on ImageJ software and normalized to the respective GAPDH signal. Whether membranes needed to be reprobed to use another antibody, stripping membrane was performed using 10 M NaOH buffer. One (n = 1) biological replicate per group, which corresponded to twenty 4-dpf larvae, was extracted in each independent experiment. At least four (N = 4) independent experiments were used for protein expression analysis.

Procedures for Zebrafish mRNA Expression Analysis

Total RNA content of at least ten 4-dpf affected and unaffected larvae were separately isolated using TRIzol reagent protocol (Invitrogen). RNA concentration was determined using a NanoDrop instrument (Thermo Fisher Scientific), and cDNA synthesis was performed using a SuperScript first-strand synthesis system (Invitrogen). TaqMan real-time PCR in triplicate technical replicates was performed using a *pitpnaa* TaqMan gene expression assay (Dr03088095_g1, Thermo Scientific) and an *hprt1* TaqMan endogenous gene expression control assay (Dr03095135_m1, Thermo Scientific) with TaqMan gene expression master mix (Thermo Scientific) and detected in the Boston Children's Hospital Molecular Genetics Core Facility using a CFX96 touch system (Bio-Rad). *pitpnaa* Ct values were normalized to respective *hprt1* Ct values. One (n = 1) biological replicate per group, which corresponded to ten 4-dpf larvae, was used in each independent experiment. Each biological replicate was used for TaqMan real-time PCR in triplicate technical replicates within at least five (N = 5) independent experiments.

Assessment of Zebrafish Locomotor Activity

Affected and unaffected 4-dpf larvae were randomly placed on 48-well plates with one larva/well. At 5 dpf, plates were placed in a DanioVision observation chamber (Noldus) and larvae were acclimated for 30 min in the dark at 28.5°C. Since the locomotor activity of juvenile zebrafish changes under light/dark conditions,[50–52] a 30-min light period followed by a 30-min dark period were then applied as presented in Figure 4A. The total distance each larvae swam (mm) and the maximum acceleration capacity (mm/s^2) of the larvae were calculated by the EthoVision XT tracking software (Noldus). Larvae were subsequently genotyped as described above. From 90 to 230 (n = 90–230) larvae were analyzed per group within at least four (N = 4) independent experiments.

Assessment of Zebrafish Muscle Force Production

Affected and unaffected larvae (6 and 7 dpf) were anesthetized in tricaine, the head of each larva was removed and stored for genotyping, and a portion of the body was attached between a force transducer and high-speed motor using a 10-0 monofilament. The attachment points were at the gastrointestinal opening and several myotomes proximal from the tip of the tail (but see below). Twitches, induced by a supramaximal, 200-μs stimulus, were used to establish the optimal length for tension. Tetani were then obtained with 30-ms trains of stimuli at 300 Hz. Force was normalized to the maximum cross-sectional area of the preparation. The cross-sectional area was assumed to be elliptical and was calculated from images of the preparation's width and depth. Experiments were conducted in a fish bicarbonate buffer maintained at 25°C and continuously equilibrated with 95% O_2, 5% CO_2. Greater details concerning the methods are available in a previous publication from our laboratory.[53] The investigator was blinded as to the treatment of the larvae studied. Analysis of birefringence suggested that there may be less myofibrillar disorganization proximal to the section of the larvae originally studied. To address this possibility, a subset of experiments was conducted in which the attachment points were just distal to the yolk sac and at

the gastrointestinal opening. There were no differences in the functional results obtained from these two sets of preparations and data were combined for analysis.

Assessment of the Cardiovascular Activity

Affected and unaffected 5-dpf larvae were anesthetized with 0.02% tricaine (MS-222, Sigma-Aldrich) since this concentration does not affect cardiac function of juvenile zebrafish, as previously described.[90] On a thin layer of 2% gelatin/E2 water, larvae were positioned under a Nikon SMZ1500 stereomicroscope. Heart rate and the posterior cardinal vein were visualized through the transparent body of the larvae and were recorded for at least 30 s at 28°C using a Basler acA1300-60gm camera (100 frames/s, 1,024 × 768 pixels). Heart beats per minute were determined manually after recording, while the blood flow of the posterior cardinal vein (arbitrary unit) were determined by drawing three random arenas of measurement along the vein in DanioScope software (Noldus). Larvae were subsequently genotyped as described above. From 10 to 22 (n = 10–22) larvae were analyzed per group within at least three (N = 3) independent experiments.

Human Samples

Human tissue was collected under the protocol #03-12-205R approved by the Committee of Clinical Investigation at Boston Children's Hospital. All patients gave their written consent to participate. Tissue from two patients with DMD was snap-frozen and primary muscle cells were dissociated and purified following CD56 fluorescence-activated cell sorting (FACS) sorting, as previously described.[91] Human myoblasts were cultured on plates coated with 0.1% gelatin in proliferation medium (20% fetal bovine serum, 1% penicillin-streptomycin-glutamine, DMEM with 4.5 g of glucose, Gibco) until 90% confluence and then switched to differentiation medium (2% horse serum, 1% penicillin-streptomycin-glutamine, DMEM with 1 g of glucose, Gibco) in 5% CO_2-humidified atmosphere at 37°C as previously described.[91] Pharmacological treatments that included PDE10A inhibitor PF-02545920 at a concentration of 25 μM in the presence of 0.25% DMSO (#D5879, Sigma-Aldrich) were applied to myoblasts under proliferation or to differentiated culture (day 6) for 24 h (concentration and duration of treatment have been selected based on different cell-based experiments that effectively used PF-02545920 compound[65,84,92]). Cells were then rinsed three times with cold PBS and scrapped in cold radioimmunoprecipitation assay (RIPA) buffer (Boston BioProducts) containing anti-proteases (cOmplete, mini, EDTA-free, Roche) and anti-phosphatases (PhosSTOP, Sigma-Aldrich). Procedures for protein expression analysis are described above. Anti-PITPNA (1:1,000, sab1400211, Sigma-Aldrich) and anti-GAPDH (1:50,000, sc-47724, Santa Cruz Biotechnology) primary antibodies were used. Protein signal intensities were analyzed on ImageJ software and normalized to respective GAPDH signal. Cells were also then rinsed three times with cold PBS and total RNA was isolated using TRIzol reagent protocol (Invitrogen). Procedures for mRNA expression analysis are described above. A *PITPNA* TaqMan gene expression assay (Hs00737576_m1, Thermo Scientific) and *GAPDH* TaqMan gene expression assay (Hs02786624_g1, Thermo Scientific) were used for TaqMan real-time PCR. *PITPNA* Ct values were normalized to respective *GAPDH* Ct values. At least nine (n = 9) biological replicates were used within three (N = 3) independent experiments for each experimental treatment. Each biological replicate for TaqMan real-time PCR was run in triplicate technical replicates.

Statistical Analysis

For the small-molecule experiments, experimental treatments were compared to the internal DMSO control group. For the morpholino experiments, morphant groups were compared to internal respective uninjected groups from the same cohort. All results (except for the long-term survival assay) were shown as means ± SEM. Statistical analyses of the data were performed using GraphPad Prism to implement a Student's t test (or log-rank test for the long-term survival assay). p values of <0.05 were considered to be statistically significant.

SUPPLEMENTAL INFORMATION

Supplemental Information can be found online at https://doi.org/10.1016/j.ymthe.2020.11.021.

ACKNOWLEDGMENTS

We thank Christian Lawrence and Mitchel Shia for the maintenance of environmental and housing zebrafish conditions, the use of equipment, and advice in the Boston Children's Hospital Aquatics Facility. We thank the BCH IDDRC Molecular Genetics Core, supported by the National Institutes of Health 1U54HD090255, for providing Sanger sequencing and the use of the CFX96 touch system (Bio-Rad) for RT-PCR. We thank Alan Beggs in the Division of Genetics and Genomics at Boston Children's Hospital for use of the DanioVision system (Noldus). We thank Emanuela Gussoni in the Division of Genetics and Genomics at Boston Children's Hospital for intellectual input and valuable comments. Funding for this work was provided by the National Institutes of Health R01AR064300 (to L.M.K), Pfizer (to L.M.K), and by the Bernard F. and Alva B. Gimbel Foundation (to L.M.K). M.R.L was supported by AFM-Téléthon (post-doctoral fellowship 21904).

AUTHOR CONTRIBUTIONS

Conceptualization, M.R.L., J.M.S., J.E.C., J.M.O., and L.M.K.; Methodology, M.R.L., J.M.S., J.J.W., A.P., J.R.C., and L.M.K.; Investigation, M.R.L., J.M.S. and J.J.W.; Formal Analysis, M.R.L.; Visualization, M.R.L.; Writing – Original Draft, M.R.L. and L.M.K.; Funding Acquisition, L.M.K. and M.R.L.; Supervision: J.E.C., J.M.O., and L.M.K.

DECLARATION OF INTERESTS

L.M.K is a consultant for Pfizer, Dyne Therapeutics, and Myofinity for muscle disease drug therapies. J.E.C and J.M.O are employees of Pfizer. The remaining authors declare no competing interests.

REFERENCES

1. Koenig, M., Hoffman, E.P., Bertelson, C.J., Monaco, A.P., Feener, C., and Kunkel, L.M. (1987). Complete cloning of the Duchenne muscular dystrophy (DMD) cDNA and preliminary genomic organization of the DMD gene in normal and affected individuals. Cell *50*, 509–517.

2. Bladen, C.L., Salgado, D., Monges, S., Foncuberta, M.E., Kekou, K., Kosma, K., Dawkins, H., Lamont, L., Roy, A.J., Chamova, T., et al. (2015). The TREAT-NMD DMD global database: analysis of more than 7,000 Duchenne muscular dystrophy mutations. Hum. Mutat. *36*, 395–402.

3. Hoffman, E.P., Brown, R.H., Jr., and Kunkel, L.M. (1987). Dystrophin: the protein product of the Duchenne muscular dystrophy locus. Cell *51*, 919–928.

4. Straub, V., Bittner, R.E., Léger, J.J., and Voit, T. (1992). Direct visualization of the dystrophin network on skeletal muscle fiber membrane. J. Cell Biol. *119*, 1183–1191.

5. Ervasti, J.M., and Campbell, K.P. (1991). Membrane organization of the dystrophin-glycoprotein complex. Cell *66*, 1121–1131.

6. Guiraud, S., Aartsma-Rus, A., Vieira, N.M., Davies, K.E., van Ommen, G.-J.B., and Kunkel, L.M. (2015). The pathogenesis and therapy of muscular dystrophies. Annu. Rev. Genomics Hum. Genet. *16*, 281–308.

7. Allen, D.G., Whitehead, N.P., and Froehner, S.C. (2016). Absence of dystrophin disrupts skeletal muscle signaling: roles of Ca^{2+}, reactive oxygen species, and nitric oxide in the development of muscular dystrophy. Physiol. Rev. *96*, 253–305.

8. Consolino, C.M., and Brooks, S.V. (2004). Susceptibility to sarcomere injury induced by single stretches of maximally activated muscles of *mdx* mice. J Appl Physiol (1985) *96*, 633–638.

9. Mendell, J.R., Shilling, C., Leslie, N.D., Flanigan, K.M., al-Dahhak, R., Gastier-Foster, J., Kneile, K., Dunn, D.M., Duval, B., Aoyagi, A., et al. (2012). Evidence-based path to newborn screening for Duchenne muscular dystrophy. Ann. Neurol. *71*, 304–313.

10. Mah, J.K., Korngut, L., Dykeman, J., Day, L., Pringsheim, T., and Jette, N. (2014). A systematic review and meta-analysis on the epidemiology of Duchenne and Becker muscular dystrophy. Neuromuscul. Disord. *24*, 482–491.

11. Emery, A.E.H., Muntoni, F., and Quinlivan, R.C.M. (2015). Duchenne Muscular Dystrophy, Fourth Edition (Oxford University Press).

12. Ryder, S., Leadley, R.M., Armstrong, N., Westwood, M., de Kock, S., Butt, T., Jain, M., and Kleijnen, J. (2017). The burden, epidemiology, costs and treatment for Duchenne muscular dystrophy: an evidence review. Orphanet J. Rare Dis. *12*, 79.

13. Kamdar, F., and Garry, D.J. (2016). Dystrophin-deficient cardiomyopathy. J. Am. Coll. Cardiol. *67*, 2533–2546.

14. Hightower, R.M., and Alexander, M.S. (2018). Genetic modifiers of Duchenne and facioscapulohumeral muscular dystrophies. Muscle Nerve *57*, 6–15.

15. Pegoraro, E., Hoffman, E.P., Piva, L., Gavassini, B.F., Cagnin, S., Ermani, M., Bello, L., Soraru, G., Pacchioni, B., Bonifati, M.D., et al.; Cooperative International Neuromuscular Research Group (2011). SPP1 genotype is a determinant of disease severity in Duchenne muscular dystrophy. Neurology *76*, 219–226.

16. Flanigan, K.M., Ceco, E., Lamar, K.M., Kaminoh, Y., Dunn, D.M., Mendell, J.R., King, W.M., Pestronk, A., Florence, J.M., Mathews, K.D., et al.; United Dystrophinopathy Project (2013). *LTBP4* genotype predicts age of ambulatory loss in Duchenne muscular dystrophy. Ann. Neurol. *73*, 481–488.

17. Bello, L., Kesari, A., Gordish-Dressman, H., Cnaan, A., Morgenroth, L.P., Punetha, J., Duong, T., Henricson, E.K., Pegoraro, E., McDonald, C.M., and Hoffman, E.P.; Cooperative International Neuromuscular Research Group Investigators (2015). Genetic modifiers of ambulation in the Cooperative International Neuromuscular Research Group Duchenne Natural History Study. Ann. Neurol. *77*, 684–696.

18. Bello, L., Flanigan, K.M., Weiss, R.B., Spitali, P., Aartsma-Rus, A., Muntoni, F., Zaharieva, I., Ferlini, A., Mercuri, E., Tuffery-Giraud, S., et al.; United Dystrophinopathy Project; Cooperative International Neuromuscular Research Group (2016). Association study of exon variants in the NF-κB and TGFβ pathways identifies CD40 as a modifier of Duchenne muscular dystrophy. Am. J. Hum. Genet. *99*, 1163–1171.

19. Hogarth, M.W., Houweling, P.J., Thomas, K.C., Gordish-Dressman, H., Bello, L., Pegoraro, E., Hoffman, E.P., Head, S.I., and North, K.N.; Cooperative International Neuromuscular Research Group (CINRG) (2017). Evidence for *ACTN3* as a genetic modifier of Duchenne muscular dystrophy. Nat. Commun. *8*, 14143.

20. Spitali, P., Zaharieva, I., Bohringer, S., Hiller, M., Chaouch, A., Roos, A., Scotton, C., Claustres, M., Bello, L., McDonald, C.M., et al.; CINRG Investigators (2020). TCTEX1D1 is a genetic modifier of disease progression in Duchenne muscular dystrophy. Eur. J. Hum. Genet. *28*, 815–825.

21. Tinsley, J., Deconinck, N., Fisher, R., Kahn, D., Phelps, S., Gillis, J.M., and Davies, K. (1998). Expression of full-length utrophin prevents muscular dystrophy in mdx mice. Nat. Med. *4*, 1441–1444.

22. Amenta, A.R., Yilmaz, A., Bogdanovich, S., McKechnie, B.A., Abedi, M., Khurana, T.S., and Fallon, J.R. (2011). Biglycan recruits utrophin to the sarcolemma and counters dystrophic pathology in mdx mice. Proc. Natl. Acad. Sci. USA *108*, 762–767.

23. Acuña, M.J., Pessina, P., Olguin, H., Cabrera, D., Vio, C.P., Bader, M., Muñoz-Canoves, P., Santos, R.A., Cabello-Verrugio, C., and Brandan, E. (2014). Restoration of muscle strength in dystrophic muscle by angiotensin-1-7 through inhibition of TGF-β signalling. Hum. Mol. Genet. *23*, 1237–1249.

24. Swaggart, K.A., Demonbreun, A.R., Vo, A.H., Swanson, K.E., Kim, E.Y., Fahrenbach, J.P., Holley-Cuthrell, J., Eskin, A., Chen, Z., Squire, K., et al. (2014). Annexin A6 modifies muscular dystrophy by mediating sarcolemmal repair. Proc. Natl. Acad. Sci. USA *111*, 6004–6009.

25. Van Ry, P.M., Wuebbles, R.D., Key, M., and Burkin, D.J. (2015). Galectin-1 protein therapy prevents pathology and improves muscle function in the mdx mouse model of Duchenne muscular dystrophy. Mol. Ther. *23*, 1285–1297.

26. Marshall, J.L., Oh, J., Chou, E., Lee, J.A., Holmberg, J., Burkin, D.J., and Crosbie-Watson, R.H. (2015). Sarcospan integration into laminin-binding adhesion complexes that ameliorate muscular dystrophy requires utrophin and α7 integrin. Hum. Mol. Genet. *24*, 2011–2022.

27. Vetrone, S.A., Montecino-Rodriguez, E., Kudryashova, E., Kramerova, I., Hoffman, E.P., Liu, S.D., Miceli, M.C., and Spencer, M.J. (2009). Osteopontin promotes fibrosis in dystrophic mouse muscle by modulating immune cell subsets and intramuscular TGF-β. J. Clin. Invest. *119*, 1583–1594.

28. Vieira, N.M., Elvers, I., Alexander, M.S., Moreira, Y.B., Eran, A., Gomes, J.P., Marshall, J.L., Karlsson, E.K., Verjovski-Almeida, S., Lindblad-Toh, K., et al. (2015). Jagged 1 rescues the Duchenne muscular dystrophy phenotype. Cell *163*, 1204–1213.

29. Vieira, N.M., Spinazzola, J.M., Alexander, M.S., Moreira, Y.B., Kawahara, G., Gibbs, D.E., Mead, L.C., Verjovski-Almeida, S., Zatz, M., and Kunkel, L.M. (2017). Repression of phosphatidylinositol transfer protein α ameliorates the pathology of Duchenne muscular dystrophy. Proc. Natl. Acad. Sci. USA *114*, 6080–6085.

30. Ambrósio, C.E., Valadares, M.C., Zucconi, E., Cabral, R., Pearson, P.L., Gaiad, T.P., Canovas, M., Vainzof, M., Miglino, M.A., and Zatz, M. (2008). Ringo, a golden retriever muscular dystrophy (GRMD) dog with absent dystrophin but normal strength. Neuromuscul. Disord. *18*, 892–893.

31. Zucconi, E., Valadares, M.C., Vieira, N.M., Bueno, C.R., Jr., Secco, M., Jazedje, T., da Silva, H.C., Vainzof, M., and Zatz, M. (2010). Ringo: discordance between the molecular and clinical manifestation in a golden retriever muscular dystrophy dog. Neuromuscul. Disord. *20*, 64–70.

32. Zatz, M., Vieira, N.M., Zucconi, E., Pelatti, M., Gomes, J., Vainzof, M., Martins-Bach, A.B., Garcia Otaduy, M.C., Bento dos Santos, G., Amaro, E., Jr., et al. (2015). A normal life without muscle dystrophin. Neuromuscul. Disord. *25*, 371–374.

33. Li, M., Hromowyk, K.J., Amacher, S.L., and Currie, P.D. (2017). Muscular dystrophy modeling in zebrafish. Methods Cell Biol. *138*, 347–380.

34. Widrick, J.J., Kawahara, G., Alexander, M.S., Beggs, A.H., and Kunkel, L.M. (2019). Discovery of novel therapeutics for muscular dystrophies using zebrafish phenotypic screens. J. Neuromuscul. Dis. *6*, 271–287.

35. Granato, M., van Eeden, F.J., Schach, U., Trowe, T., Brand, M., Furutani-Seiki, M., Haffter, P., Hammerschmidt, M., Heisenberg, C.P., Jiang, Y.J., et al. (1996). Genes controlling and mediating locomotion behavior of the zebrafish embryo and larva. Development *123*, 399–413.

36. Bassett, D.I., Bryson-Richardson, R.J., Daggett, D.F., Gautier, P., Keenan, D.G., and Currie, P.D. (2003). Dystrophin is required for the formation of stable muscle attachments in the zebrafish embryo. Development *130*, 5851–5860.

37. Bassett, D., and Currie, P.D. (2004). Identification of a zebrafish model of muscular dystrophy. Clin. Exp. Pharmacol. Physiol. *31*, 537–540.

38. Guyon, J.R., Goswami, J., Jun, S.J., Thorne, M., Howell, M., Pusack, T., Kawahara, G., Steffen, L.S., Galdzicki, M., and Kunkel, L.M. (2009). Genetic isolation and characterization of a splicing mutant of zebrafish dystrophin. Hum. Mol. Genet. *18*, 202–211.

39. Kawahara, G., Karpf, J.A., Myers, J.A., Alexander, M.S., Guyon, J.R., and Kunkel, L.M. (2011). Drug screening in a zebrafish model of Duchenne muscular dystrophy. Proc. Natl. Acad. Sci. USA *108*, 5331–5336.

40. Kawahara, G., and Kunkel, L.M. (2013). Zebrafish based small molecule screens for novel DMD drugs. Drug Discov. Today Technol. *10*, e91–e96.

41. Kawahara, G., Gasperini, M.J., Myers, J.A., Widrick, J.J., Eran, A., Serafini, P.R., Alexander, M.S., Pletcher, M.T., Morris, C.A., and Kunkel, L.M. (2014). Dystrophic muscle improvement in zebrafish via increased heme oxygenase signaling. Hum. Mol. Genet. *23*, 1869–1878.

42. Waugh, T.A., Horstick, E., Hur, J., Jackson, S.W., Davidson, A.E., Li, X., and Dowling, J.J. (2014). Fluoxetine prevents dystrophic changes in a zebrafish model of Duchenne muscular dystrophy. Hum. Mol. Genet. *23*, 4651–4662.

43. Hightower, R.M., Reid, A.L., Gibbs, D.E., Wang, Y., Widrick, J.J., Kunkel, L.M., Kastenschmidt, J.M., Villalta, S.A., van Groen, T., Chang, H., et al. (2020). The SINE compound KPT-350 blocks dystrophic pathologies in DMD zebrafish and mice. Mol. Ther. *28*, 189–201.

44. Farr, G.H., 3rd, Morris, M., Gomez, A., Pham, T., Kilroy, E., Parker, E.U., Said, S., Henry, C., and Maves, L. (2020). A novel chemical-combination screen in zebrafish identifies epigenetic small molecule candidates for the treatment of Duchenne muscular dystrophy. Skelet. Muscle *10*, 29.

45. Percival, J.M., Whitehead, N.P., Adams, M.E., Adamo, C.M., Beavo, J.A., and Froehner, S.C. (2012). Sildenafil reduces respiratory muscle weakness and fibrosis in the *mdx* mouse model of Duchenne muscular dystrophy. J. Pathol. *228*, 77–87.

46. Leung, D.G., Herzka, D.A., Thompson, W.R., He, B., Bibat, G., Tennekoon, G., Russell, S.D., Schuleri, K.H., Lardo, A.C., Kass, D.A., et al. (2014). Sildenafil does not improve cardiomyopathy in Duchenne/Becker muscular dystrophy. Ann. Neurol. *76*, 541–549.

47. Nelson, M.D., Rader, F., Tang, X., Tavyev, J., Nelson, S.F., Miceli, M.C., Elashoff, R.M., Sweeney, H.L., and Victor, R.G. (2014). PDE5 inhibition alleviates functional muscle ischemia in boys with Duchenne muscular dystrophy. Neurology *82*, 2085–2091.

48. Spinazzola, J.M., Lambert, M.R., Gibbs, D.E., Conner, J.R., Krikorian, G.L., Pareek, P., Rago, C., and Kunkel, L.M. (2020). Effect of serotonin modulation on dystrophin-deficient zebrafish. Biol. Open *9*, bio053363.

49. Berger, J., Sztal, T., and Currie, P.D. (2012). Quantification of birefringence readily measures the level of muscle damage in zebrafish. Biochem. Biophys. Res. Commun. *423*, 785–788.

50. Burgess, H.A., and Granato, M. (2007). Modulation of locomotor activity in larval zebrafish during light adaptation. J. Exp. Biol. *210*, 2526–2539.

51. Emran, F., Rihel, J., and Dowling, J.E. (2008). A behavioral assay to measure responsiveness of zebrafish to changes in light intensities. J. Vis. Exp. (20), 923.

52. Basnet, R.M., Zizioli, D., Taweedet, S., Finazzi, D., and Memo, M. (2019). Zebrafish larvae as a behavioral model in neuropharmacology. Biomedicines *7*, 23.

53. Widrick, J.J., Alexander, M., Sanchez, B., Gibbs, D., Kawahara, G., Beggs, A., and Kunkel, L. (2016). Muscle dysfunction in a zebrafish model of Duchenne muscular dystrophy. Physiol. Genomics *48*, 850–860.

54. Chen, J. (2013). Impaired cardiovascular function caused by different stressors elicits a common pathological and transcriptional response in zebrafish embryos. Zebrafish *10*, 389–400.

55. Azevedo, M.F., Faucz, F.R., Bimpaki, E., Horvath, A., Levy, I., de Alexandre, R.B., Ahmad, F., Manganiello, V., and Stratakis, C.A. (2014). Clinical and molecular genetics of the phosphodiesterases (PDEs). Endocr. Rev. *35*, 195–233.

56. Baillie, G.S., Tejeda, G.S., and Kelly, M.P. (2019). Therapeutic targeting of 3′,5′-cyclic nucleotide phosphodiesterases: inhibition and beyond. Nat. Rev. Drug Discov. *18*, 770–796.

57. Bloom, T.J. (2002). Cyclic nucleotide phosphodiesterase isozymes expressed in mouse skeletal muscle. Can. J. Physiol. Pharmacol. *80*, 1132–1135.

58. Bloom, T.J. (2005). Age-related alterations in cyclic nucleotide phosphodiesterase activity in dystrophic mouse leg muscle. Can. J. Physiol. Pharmacol. *83*, 1055–1060.

59. Mishra, S.K., Menon, N.K., Roman, D., and Kumar, S. (1992). Calcium, calmodulin and 3′,5′-cyclic nucleotide phosphodiesterase activity in human muscular disorders. J. Neurol. Sci. *109*, 215–218.

60. Stapleton, D.I., Lau, X., Flores, M., Trieu, J., Gehrig, S.M., Chee, A., Naim, T., Lynch, G.S., and Koopman, R. (2014). Dysfunctional muscle and liver glycogen metabolism in *mdx* dystrophic mice. PLoS One *9*, e91514.

61. Percival, J.M., Adamo, C.M., Beavo, J.A., and Froehner, S.C. (2011). Evaluation of the therapeutic utility of phosphodiesterase 5A inhibition in the *mdx* mouse model of Duchenne muscular dystrophy. Handb. Exp. Pharmacol. (204), 323–344.

62. Nio, Y., Tanaka, M., Hirozane, Y., Muraki, Y., Okawara, M., Hazama, M., and Matsuo, T. (2017). Phosphodiesterase 4 inhibitor and phosphodiesterase 5 inhibitor combination therapy has antifibrotic and anti-inflammatory effects in mdx mice with Duchenne muscular dystrophy. FASEB J. *31*, 5307–5320.

63. Hankir, M.K., Kranz, M., Gnad, T., Weiner, J., Wagner, S., Deuther-Conrad, W., Bronisch, F., Steinhoff, K., Luthardt, J., Klöting, N., et al. (2016). A novel thermoregulatory role for PDE10A in mouse and human adipocytes. EMBO Mol. Med. *8*, 796–812.

64. Genders, A.J., Bradley, E.A., Rattigan, S., and Richards, S.M. (2011). cGMP phosphodiesterase inhibition improves the vascular and metabolic actions of insulin in skeletal muscle. Am. J. Physiol. Endocrinol. Metab. *301*, E342–E350.

65. Chen, S., Zhang, Y., Lighthouse, J.K., Mickelsen, D.M., Wu, J., Yao, P., Small, E.M., and Yan, C. (2020). A novel role of cyclic nucleotide phosphodiesterase 10A in pathological cardiac remodeling and dysfunction. Circulation *141*, 217–233.

66. Adamo, C.M., Dai, D.F., Percival, J.M., Minami, E., Willis, M.S., Patrucco, E., Froehner, S.C., and Beavo, J.A. (2010). Sildenafil reverses cardiac dysfunction in the mdx mouse model of Duchenne muscular dystrophy. Proc. Natl. Acad. Sci. USA *107*, 19079–19083.

67. De Arcangelis, V., Strimpakos, G., Gabanella, F., Corbi, N., Luvisetto, S., Magrelli, A., Onori, A., Passananti, C., Pisani, C., Rome, S., et al. (2016). Pathways implicated in tadalafil amelioration of duchenne muscular dystrophy. J. Cell. Physiol. *231*, 224–232.

68. Hammers, D.W., Sleeper, M.M., Forbes, S.C., Shima, A., Walter, G.A., and Sweeney, H.L. (2016). Tadalafil treatment delays the onset of cardiomyopathy in dystrophin-deficient hearts. J. Am. Heart Assoc. *5*, e003911.

69. Batra, A., Vohra, R.S., Chrzanowski, S.M., Hammers, D.W., Lott, D.J., Vandenborne, K., Walter, G.A., and Forbes, S.C. (2019). Effects of PDE5 inhibition on dystrophic muscle following an acute bout of downhill running and endurance training. J Appl Physiol (1985) *126*, 1737–1745.

70. Victor, R.G., Sweeney, H.L., Finkel, R., McDonald, C.M., Byrne, B., Eagle, M., Goemans, N., Vandenborne, K., Dubrovsky, A.L., Topaloglu, H., et al.; Tadalafil DMD Study Group (2017). A phase 3 randomized placebo-controlled trial of tadalafil for Duchenne muscular dystrophy. Neurology *89*, 1811–1820.

71. Dietz, A.R., Connolly, A., Dori, A., and Zaidman, C.M. (2020). Intramuscular blood flow in Duchenne and Becker muscular dystrophy: quantitative power Doppler sonography relates to disease severity. Clin. Neurophysiol. *131*, 1–5.

72. Serafini, P.R., Feyder, M.J., Hightower, R.M., Garcia-Perez, D., Vieira, N.M., Lek, A., Gibbs, D.E., Moukha-Chafiq, O., Augelli-Szafran, C.E., Kawahara, G., et al. (2018). A limb-girdle muscular dystrophy 2I model of muscular dystrophy identifies corrective drug compounds for dystroglycanopathies. JCI Insight *3*, e120493.

73. Eisen, J.S., and Smith, J.C. (2008). Controlling morpholino experiments: don't stop making antisense. Development *135*, 1735–1743.

74. Cockcroft, S. (2007). Trafficking of phosphatidylinositol by phosphatidylinositol transfer proteins. Biochem. Soc. Symp. *74*, 259–271.

75. Phillips, S.E., Vincent, P., Rizzieri, K.E., Schaaf, G., Bankaitis, V.A., and Gaucher, E.A. (2006). The diverse biological functions of phosphatidylinositol transfer proteins in eukaryotes. Crit. Rev. Biochem. Mol. Biol. *41*, 21–49.

76. Baptist, M., Panagabko, C., Cockcroft, S., and Atkinson, J. (2016). Ligand and membrane-binding behavior of the phosphatidylinositol transfer proteins PITPα and PITPβ. Biochem. Cell Biol. *94*, 528–533.

77. Kim, M.H., Kay, D.I., Rudra, R.T., Chen, B.M., Hsu, N., Izumiya, Y., Martinez, L., Spencer, M.J., Walsh, K., Grinnell, A.D., and Crosbie, R.H. (2011). Myogenic Akt signaling attenuates muscular degeneration, promotes myofiber regeneration and improves muscle function in dystrophin-deficient mdx mice. Hum. Mol. Genet. *20*, 1324–1338.

78. Peter, A.K., Ko, C.Y., Kim, M.H., Hsu, N., Ouchi, N., Rhie, S., Izumiya, Y., Zeng, L., Walsh, K., and Crosbie, R.H. (2009). Myogenic Akt signaling upregulates the

utrophin-glycoprotein complex and promotes sarcolemma stability in muscular dystrophy. Hum. Mol. Genet. *18*, 318–327.

79. Marshall, J.L., Holmberg, J., Chou, E., Ocampo, A.C., Oh, J., Lee, J., Peter, A.K., Martin, P.T., and Crosbie-Watson, R.H. (2012). Sarcospan-dependent Akt activation is required for utrophin expression and muscle regeneration. J. Cell Biol. *197*, 1009–1027.

80. Alexander, M.S., Casar, J.C., Motohashi, N., Vieira, N.M., Eisenberg, I., Marshall, J.L., Gasperini, M.J., Lek, A., Myers, J.A., Estrella, E.A., et al. (2014). MicroRNA-486-dependent modulation of DOCK3/PTEN/AKT signaling pathways improves muscular dystrophy-associated symptoms. J. Clin. Invest. *124*, 2651–2667.

81. Peter, A.K., and Crosbie, R.H. (2006). Hypertrophic response of Duchenne and limb-girdle muscular dystrophies is associated with activation of Akt pathway. Exp. Cell Res. *312*, 2580–2591.

82. Blaauw, B., Mammucari, C., Toniolo, L., Agatea, L., Abraham, R., Sandri, M., Reggiani, C., and Schiaffino, S. (2008). Akt activation prevents the force drop induced by eccentric contractions in dystrophin-deficient skeletal muscle. Hum. Mol. Genet. *17*, 3686–3696.

83. Takahashi, A., Kureishi, Y., Yang, J., Luo, Z., Guo, K., Mukhopadhyay, D., Ivashchenko, Y., Branellec, D., and Walsh, K. (2002). Myogenic Akt signaling regulates blood vessel recruitment during myofiber growth. Mol. Cell. Biol. *22*, 4803–4814.

84. Li, N., Lee, K., Xi, Y., Zhu, B., Gary, B.D., Ramírez-Alcántara, V., Gurpinar, E., Canzoneri, J.C., Fajardo, A., Sigler, S., et al. (2015). Phosphodiesterase 10A: a novel target for selective inhibition of colon tumor cell growth and β-catenin-dependent TCF transcriptional activity. Oncogene *34*, 1499–1509.

85. Alb, J.G., Jr., Cortese, J.D., Phillips, S.E., Albin, R.L., Nagy, T.R., Hamilton, B.A., and Bankaitis, V.A. (2003). Mice lacking phosphatidylinositol transfer protein-α exhibit spinocerebellar degeneration, intestinal and hepatic steatosis, and hypoglycemia. J. Biol. Chem. *278*, 33501–33518.

86. Spinazzola, J.M., and Kunkel, L.M. (2016). Pharmacological therapeutics targeting the secondary defects and downstream pathology of Duchenne muscular dystrophy. Expert Opin. Orphan Drugs *4*, 1179–1194.

87. Malamas, M.S., Ni, Y., Erdei, J., Stange, H., Schindler, R., Lankau, H.-J., Grunwald, C., Fan, K.Y., Parris, K., Langen, B., et al. (2011). Highly potent, selective, and orally active phosphodiesterase 10A inhibitors. J. Med. Chem. *54*, 7621–7638.

88. Verhoest, P.R., Chapin, D.S., Corman, M., Fonseca, K., Harms, J.F., Hou, X., Marr, E.S., Menniti, F.S., Nelson, F., O'Connor, R., et al. (2009). Discovery of a novel class of phosphodiesterase 10A inhibitors and identification of clinical candidate 2-[4-(1-methyl-4-pyridin-4-yl-1*H*-pyrazol-3-yl)-phenoxymethyl]-quinoline (PF-2545920) for the treatment of schizophrenia. J. Med. Chem. *52*, 5188–5196.

89. Smith, L.L., Beggs, A.H., and Gupta, V.A. (2013). Analysis of skeletal muscle defects in larval zebrafish by birefringence and touch-evoke escape response assays. J. Vis. Exp. (82), e50925.

90. Denvir, M.A., Tucker, C.S., and Mullins, J.J. (2008). Systolic and diastolic ventricular function in zebrafish embryos: influence of norepenephrine, MS-222 and temperature. BMC Biotechnol. *8*, 21.

91. Spinazzola, J.M., and Gussoni, E. (2017). Isolation of primary human skeletal muscle cells. Bio Protoc. *7*, e2591.

92. Lee, K., Lindsey, A.S., Li, N., Gary, B., Andrews, J., Keeton, A.B., and Piazza, G.A. (2016). β-Catenin nuclear translocation in colorectal cancer cells is suppressed by PDE10A inhibition, cGMP elevation, and activation of PKG. Oncotarget *7*, 5353–5365.